THA 高位脱臼

高位脱臼性股関節症に対する Smith-Petersen 進入による人工股関節置換術の中・長期成績

金治有彦，安藤謙一，中川雅人，森田充浩，加藤誠，山田治基
藤田保健衛生大学整形外科

目　的

我々は人工股関節置換術（THR）を行う際には，原則的に Hardinge approach により股関節周囲を展開している[1]．しかしながら高位脱臼性股関節症では骨頭が高位にあるため，THR を行う際に，Hardinge あるいは Dall などの anterolateral approach では展開が困難なことがある．そこでわれわれは殿筋内脱臼例などの高位脱臼性股関節症に対しては Smith-Petersen 進入による手術を行うことを第一選択としてきた．本研究の目的は Crowe 分類 group IV の高位脱臼例に対して行った Smith-Petersen 進入による THR の中・長期成績を明らかにすることである．

対象と方法

症例は 12 例で，全例女性であった．いずれの症例も Crowe 分類 group IV に分類される高位脱臼例であり，7 例は新臼蓋を形成していたが 5 例は殿筋内脱臼例であった．手術時年齢は 53 歳から 76 歳，平均 66.3 歳．術後経過観察期間は 1 年から 12 年，平均 7.5 年であった．

我々の行う Smith-Petersen 進入による手術法を以下に説明する．我々は中殿筋機能を温存することを目的として，腸骨稜外側を平ノミで屋根瓦状に骨切りし，骨膜下に中殿筋を剥離している[3,4]．一般的に高位脱臼性股関節症の症例では臼蓋後壁が非常に薄く，しかも臼蓋前後径が小さいことが特徴的である．そのため股関節周囲を充分に展開して骨盤形態を把握し，臼蓋の前後径を考慮してカップの設置位置を決定している．臼蓋骨欠損部を移植骨で補填後，カップはセメント固定することを原則としている．

以上のような方法により THR を施行した高位脱臼性股関節症の 12 例に対し，カップの大きさと設置角度，手術時間，出血量，移植骨の種類，大腿骨短縮骨切り術の有無，術前後の脚長差，術前および最終調査時の JOA hip score，股関節単純 X 線像における臼蓋カップとステムの弛みの有無を調査した．

結　果

使用したカップの大きさは 9 例が 40 mm，2 例が 42 mm，1 例が 44 mm であり，小さいカップが使用されていた．カップの外方傾斜角は 35 度から 43 度，平均 39.1 度，手術時間は 170 分から 280 分，平均 216 分であった．出血量は 472 g から 2039 g，平均 864 g．移植骨の種類は自家骨 8 例，同種骨 4 例であった．大腿骨短縮骨切り術は 12 例中 2 例に行われていた．術前の脚長差は 1.8 cm から 4.7 cm，平均 3.7 cm であったが，術後脚長差は 12 例中 11 例が 1 cm 以内であった．JOA hip score は術前平均 42.1 が術後平均 84.3 に改善していた．最終調査時の両股関節単純 X 線像では，臼蓋移植骨の圧潰を 1 例に生じたが，それ以外の 11 例では明らかな弛みの所見が認められた症例はなかった．

症例供覧

症例 1．70 歳女性（新臼蓋形成例）．平成 11 年 5 月 21 日，当院にて THR を施行した．臼蓋には 44 mm のカップを選択し，外方傾斜角 40 度，前方開角 10 度で自家骨移植を併用してカップをセメント固定した．術後 10 年の現在，両股関節単純 X 線像では，ステムおよび臼蓋カップに明らかな弛みの所見は認められない（図 1）．

症例 2．60 歳女性（殿筋内脱臼例）．平成 15 年 5 月 6 日に THR を施行した．この症例では原臼位に同種骨移植を併

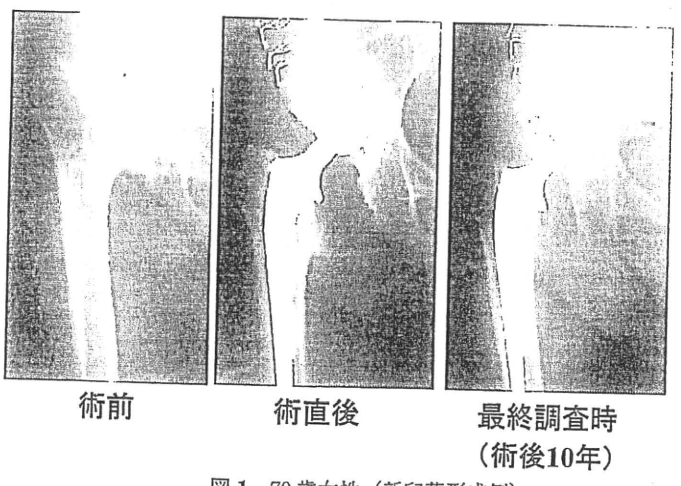

図 1　70 歳女性（新臼蓋形成例）

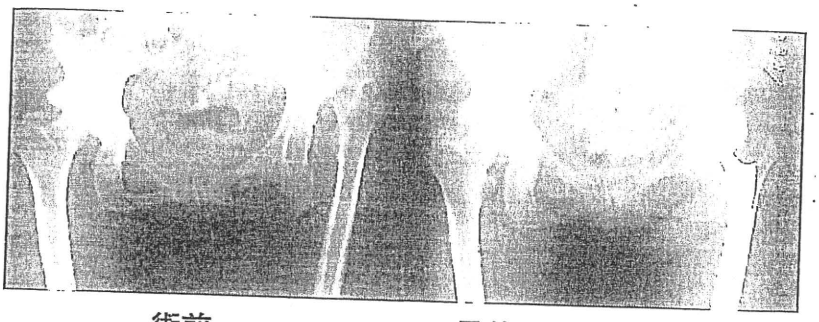

図2　60歳女性（殿筋内脱臼例）

用して40 mm径のカップをセメント固定した．カップ外方傾斜角38度，前方開角10度であり，脚長差は術前には3.7 cm存在していたが，術後の脚長差は1 cm以内である．術後6年時の両股関節単純X線像では，ステムおよび臼蓋カップに明らかな弛みの所見は認められない（図2）．

考　察

高位脱臼性股関節症に対するTHRの長期成績についてはCrowe I，IIに対するTHRと比べて不良であるとする報告が多い．Numairらは Crowe I，II，IIIに対するTHRと比べて臼蓋コンポートネントの再置換率が倍であり，15年累積生存率は68%であると報告した[5]．またHartofilakidisらは7年以上の経過でカップ再置換率が14%，ステム再置換率が16%であり，15年累積生存率は76%であったと報告した[6]．これに対してのわれわれのSmith-Petersen進入によるTHRの術後成績は術後経過観察期間が7.5年であったものの概ね良好であった．

高位脱臼性股関節症に対するTHRにおいて良好な長期成績を獲得するためには，周到な術前計画を立て，その計画通りの正確な手術を行うことが重要である．我々はCrowe分類group IVの高位脱臼例に対するTHRの際には，正確に臼蓋カップを設置することを目的として，骨盤形態を十分に観察できるSmith-Petersen進入による手術を選択している[4]．自験例では臼蓋カップの外方傾斜角は35度から43度，平均39.1度であり，全例が良好に設置されていた．この結果からSmith-Petersen進入による手術により，術前計画したとおりの正確な臼蓋カップの設置が可能であることが示された．

また高位脱臼性股関節症に対するTHRでは，骨盤の前後径の最も大きいところに充分量の良質な骨を移植し，可能な限り大きなカップを設置すべきである[4]．しかし本症では著しい臼蓋形成不全を呈する例が多いため，骨移植を行っても臼蓋カップの大きさが制限されることが多い．自験例においては，使用したセメントカップの大きさは12例中9例が40 mmであり，小さなカップが使用されていた．我々が使用した40 mmのセメントカップではポリエチレンの厚さ7 mmであり，ポリエチレンの摩耗が急速に生じた例は1例もなかったが，ポリエチレンの磨耗やそれによる骨溶解の発生に関しては，今後も長期にわたり注意深く経過観察を行う必要がある．

近年，本症に対するTHAにおいてセメントレス型人工関節の使用例が多く報告されている．しかしながらポリエチレンの厚みを念頭に置き，骨盤形態に比して大きなセメントレスカップを無理に設置しようとすると，カップの外方傾斜角が大きくなる症例や臼蓋移植骨が大きくなりすぎる症例が生じうるため，注意する必要がある．移植骨の大きさについては，移植骨によるカップの支持の割合が大きくなると移植骨が圧潰する危険性が増すため，原則としてカップの頂点を越えない大きさに留めるべきである．自験例では骨欠損の程度が大きく，止むを得ず大きな骨移植を要した1例に移植骨の圧潰を生じたが，それ以外の11例では特に問題は生じなかった．Crowe分類group IVの症例に対するTHRでは，自験例以外にも移植骨の圧潰が認められた例も報告されているため[7,8]，この点については今後も注意深く経過観察することが重要であると考えている．

結　語

1. 高位脱臼性股関節症に対するTHRでは，Smith-Petersen進入による手術により十分に骨盤形態を確認することが重要である．

2. 高位脱臼性股関節症に対するSmith-Petersen進入による手術は，術前計画したとおりの正確な手術が可能であるため，推奨できる進入法である．

文　献

1) Hardinge K: The direct lateral approach to the hip. J Bone Joint Surg Br, 64: 17-19, 1982.
2) Crowe JF, et al.: Total hip replacement in congenital dislocation and dysplasia of the hip. J Bone Joint Surg Am, 61: 15-23, 1979.
3) 安藤謙一，他：Chiari骨盤骨切り術の経験．日関外誌，10: 347-356, 1991
4) 金治有彦，他：脱臼性股関節症に対するSmith-Petersen進入による人工股関節置換術―臼蓋側の評価を中心に―．日本人工関節学会誌，35: 1-2, 2005.
5) Numair et al.: Total hip arthroplasty for congenital dislocation and dysplasia of the hip. J Bone Joint Surg Am, 79: 1352-1360, 1997.
6) Hartofilakidis, et al.: Total hip arthroplasty for congenital hip disease. J Bone Joint Surg Am, 86-A: 242-250, 2004.
7) Mulroy RD Jr, Harris WH: Failure of acetabular autogenous grafts in total hip arthroplasty. Increasing incidence: a follow-up note. J Bone Joint Surg Am, 72: 1536-1540, 1990.
8) 菅野大己，他：高位脱臼症例（Crowe III, IV）に対する初回THAの7年以上経過例の検討―臼蓋骨移植併用例―．日本人工関節学会誌，34: 71-72, 2004.

病気と薬
パーフェクトBOOK
2011

Perfect Book of Disease & Medicine

南山堂

骨・関節疾患アプローチのための解剖生理

骨格

人体の骨格は体幹と四肢から構成されている（図1）．体幹は頭蓋と脊柱，胸郭，骨盤からなり，四肢は上肢（上肢帯：上腕，前腕，手）と下肢（下肢帯：大腿，下腿，足）から成り立っている．人体は約200個の骨から構成されている．

骨の発生

骨の発生，成長形態は大腿骨のような長幹骨で認められる軟骨から形成される内軟骨性骨化と，頭蓋骨や鎖骨のように結合組織内に骨化中心ができて骨が形成される膜性骨化という2つに大別される．内軟骨性骨化では，骨の両端にある成長軟骨板（骨端軟骨板）において軟骨細胞が骨端から静止・増殖・肥大・石灰化細胞層として規則正しく配列されていて，ここで長軸方向の骨の成長が起きる（図2）．小児では長管骨骨端部の成長軟骨板で，成長とともに軟骨から骨への置換が生じる．

骨・関節の解剖

①骨・関節の形態と構造：骨格は主に骨からできており，関節でつながっていることにより動くことができる．骨の形態は長管骨，短骨，扁平骨，種子骨に分けられる．

骨の表面は骨膜で覆われており，その下には皮質骨（緻密骨）が，さらに内部には海綿骨が存在する．海綿骨は骨梁と呼ばれる規則性のある内部構造を有する．長管骨では中間部を骨幹，関節部を骨端，その境界を骨幹端と呼ぶ．骨端部と骨幹端部の境界には成長過程では成長軟骨板に相当する骨端線と呼ばれる線状影が存在するが，成長完了とともに消失する．長管骨内には髄腔というすきまがあり，これを骨髄が満たしている．骨髄には赤色骨髄と黄色骨髄があり，赤色骨髄では活発な造血機能が働

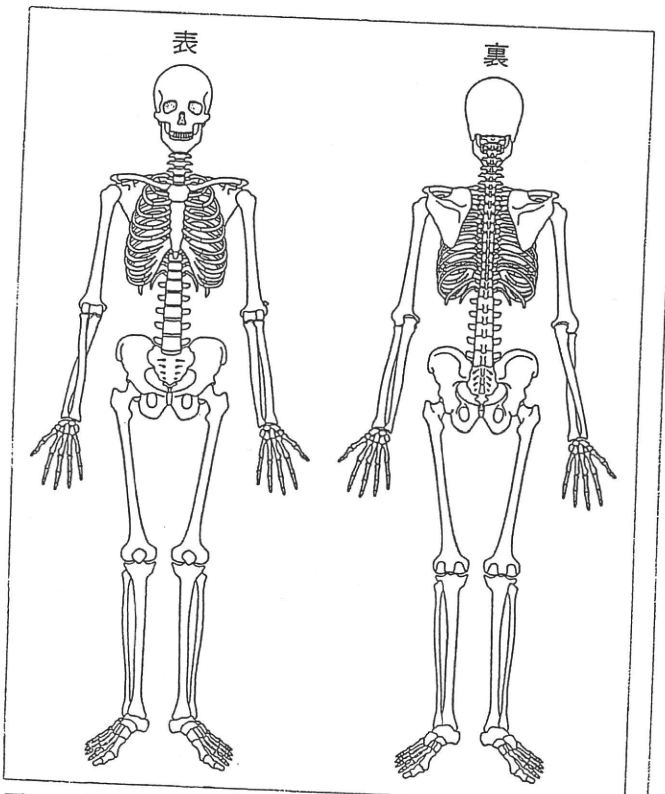

図1　骨格

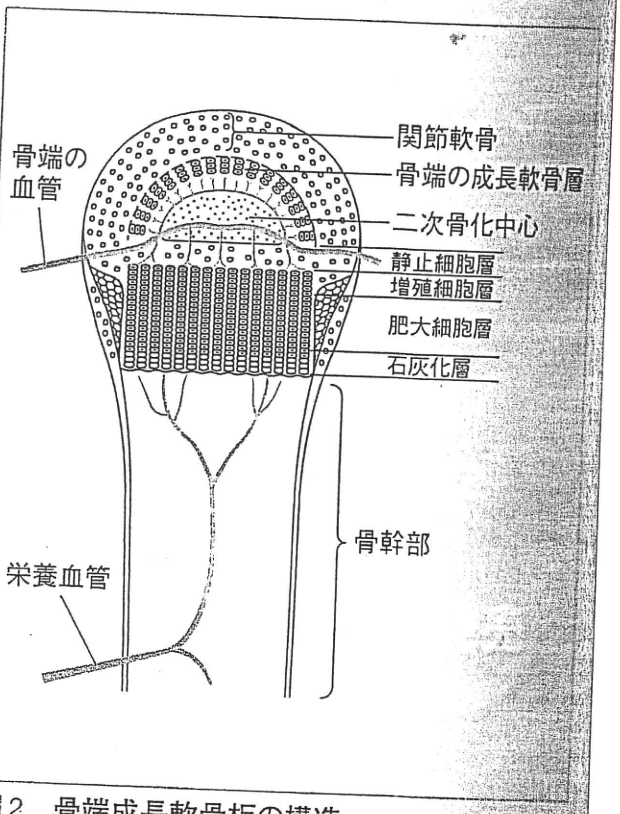

図2　骨端成長軟骨板の構造

いている．骨端は関節軟骨で覆われており，その下には軟骨下骨と呼ばれる層があって海綿骨の骨梁へ移行する．

関節は骨と骨を連結する構造体で，関節包が骨端を覆っている．関節包内には関節液（滑液）を分泌する滑膜がある．関節液は関節の動きを潤滑にするほか，関節軟骨への栄養補給などの代謝に関与している（図3）．また，補助構造物として関節唇，関節円板，半月板，靱帯などがある．

②骨・関節の組織：骨組織には骨芽細胞，破骨細胞，骨細胞が存在する．骨芽細胞は骨基質蛋白合成により骨形成を，骨細胞は細胞外液中のカルシウム濃度維持を，また破骨細胞は骨吸収の働きを有する．骨はオステオンと呼ばれる円柱状かつ同心円状の層板配列をとる骨単位から構成され，その中心には血管が通るハバース管がある．このハバース管や斜走するフォルクマン管を通じて血管が骨内部に進入する（図4）．骨の層板の間隙には骨小腔という骨細胞の入った間隙があり，骨の吸収と形成が絶え間なく行われている．

骨の固形成分はその約2/3がハイドロキシアパタイト（$Ca_{10}(PO_4)_6(OH)_2$）という無機質で，約1/3は主にコラーゲンという有機物である．有機物の95％はⅠ型コラーゲンである．

関節構成体である関節軟骨は組織学的には硝子軟骨である．成人の関節軟骨には血管や神経，リンパ管はなく，軟骨細胞と細胞外基質から成り立っている．関節軟骨はその最表層から層状に4つの層に区分されるが（図5），各境界は不明瞭である．最深層の石灰化層と，それ以外の非石灰化層のあいだにはtidemarkと呼ばれる波状の境界があり，また石灰化層は骨端の軟骨下骨と接している．関節軟骨の固形成分の約50％はコラーゲン，30～35％はアグリカンと呼ばれるプロテオグリカン，15～20％は非コラーゲン性蛋白と糖蛋白である．関節軟骨コラーゲンの約95％はⅡ型コラーゲンで，残りはⅤ，Ⅵ，Ⅸ，Ⅺ型といった微量コラーゲンである．プロテオグリカンはコア蛋白とムコ多糖（コンドロイチン硫酸とケラタン硫酸）が結合してできており，軟骨内ではさらにヒアルロン酸と結合している．

関節包はコラーゲン線維束と線維細胞からできており，その内側には滑膜が存在する．滑膜からは高分子量ヒアルロン酸を含有することにより粘稠性のある滑液が分泌され，関節軟骨間の潤滑と関節軟骨の栄養に関与している．

膝や手，顎関節などには半月板や関節円板と呼ばれる構成体が存在し，荷重に対する緩衝や関節の安定保持，潤滑などに関与している．半月板は関節軟骨と組成が類似しているものの，コラーゲンの

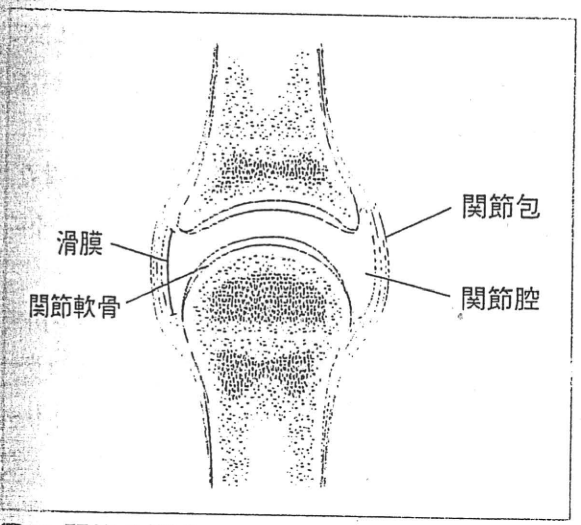

図3　関節の構造
（石橋治雄監修，田沼久美子ほか：これならわかる要点解剖学，p.28，南山堂，2004より引用）

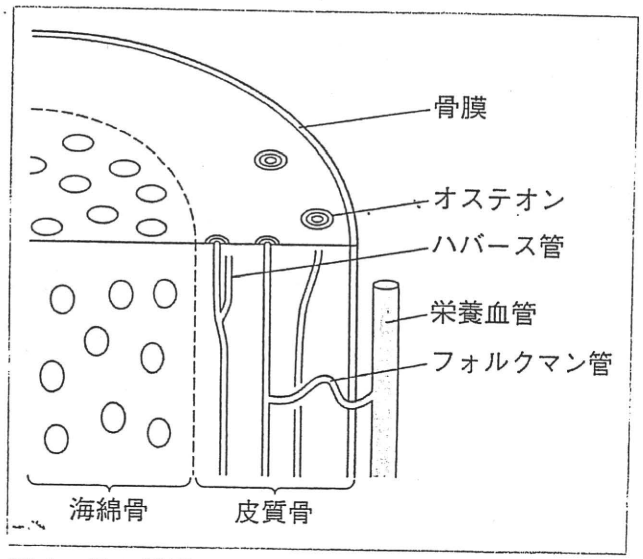

図4　骨の構造

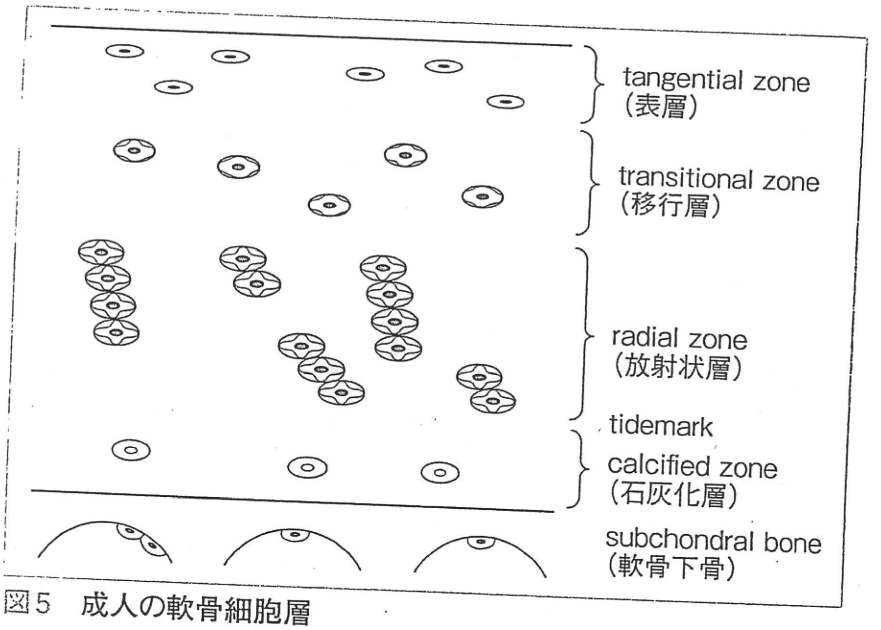

図5　成人の軟骨細胞層

90％はⅠ型コラーゲンであり，またムコ多糖もデルマタン硫酸が主である点が異なる．

骨・関節の機能

①骨の機能：骨は骨組みとして身体を支持し，筋肉によって運動するとともに，重要臓器を保護する役割をもつ．また体内カルシウムの99％を貯蔵してカルシウムバランスを保っているほか，骨髄において造血する働きをもっている．骨にはリモデリングと呼ばれる代謝機能があり，骨吸収と骨形成の機能連関によって骨形態が恒常的に維持されている．カルシウムバランスの恒常性維持には副甲状腺ホルモンやカルシトニン，エストロゲンといった内分泌ホルモンのほか，ビタミンDを代表とする各種ビタミンが密接に関わっている．

骨吸収マーカーと骨形成マーカーという骨代謝を反映する2種類のマーカーが実用化されている．骨吸収マーカーとしては尿中ピリジノリン・デオキシピリジノリン，骨型酒石酸抵抗性酸性フォスファターゼ(TRACP-5b)，血清Ⅰ型コラーゲンC末端テロペプチド(ICTP)，尿中および血清Ⅰ型コラーゲン架橋N-テロペプチド(NTX-I)などが，また骨形成マーカーとしては骨芽細胞から分泌されるオステオカルシンや骨型アルカリフォスファターゼ(BAP)，血清Ⅰ型プロコラーゲンC末端プロペプチド(PICP)，低カルボキシル化オステオカルシン(ucOC)などがあり，骨代謝回転の指標として臨床的に用いられている．

②関節の機能：関節は支持組織としての骨を連結し，円滑に動かす役割をもっている．形態学的には球関節，楕円関節，鞍関節，蝶番関節，車軸関節といった形状があり，可動関節と呼ばれる．また，頭蓋骨縫合などの線維性結合，椎間板や恥骨結合などの軟骨・靭帯性結合は可動性をもたない不動関節である．

関節の代謝は関節マーカーで評価することが可能である．軟骨マーカーにはプロテオグリカン由来成分であるコンドロイチン硫酸やケラタン硫酸，ヒアルロン酸やコラーゲン由来成分であるⅡ型コラーゲンC末端テロペプチド断片(CTX-Ⅱ)，その他の軟骨マトリックス成分である軟骨オリゴマーマトリックス蛋白(COMP)などがある．関節炎マーカーはインターロイキン-1や腫瘍壊死因子(TNF)-αなどの各種炎症性サイトカイン，蛋白分解酵素であるマトリックスメタロプロテアーゼ(MMP)，ディスインテグリンメタロプロテアーゼ(ADAM)などが知られている．現在，これらのマーカーによる関節疾患の病期病態診断などに応用するための研究が進められている．

(森田充浩／山田治基)

骨粗鬆症 osteoporosis

骨粗鬆症とは，単位体積あたりの骨量の低下と骨梁構造の悪化などにより，骨がその場に見合った物理的支持体となりえず，脆弱性が亢進し骨折危険度の高まった全身性疾患であると定義されていたが，現在では，「骨量（骨密度）と骨の質により規定される骨強度が低下したために骨折リスクの高まった状態である」と考えられている．この骨量（骨密度）以外の骨強度を決定する要因として，骨（梁）構造，骨基質のミネラル化度，コラーゲンの加齢に伴う変化，マイクロダメージの蓄積などの骨質が重要視されてきている．わが国の骨粗鬆症有病率は年齢とともに上昇し，とくに女性では60歳代後半から増加，80歳代では約半数が罹患しており，推計患者数は約800万～1,100万人とされているが，今後さらなる増加が考えられる．

治療方針の要点 CL 骨粗鬆症の予防と治療ガイドライン2006年版

- 骨粗鬆症治療の目的は，骨折の危険性を抑制し，QOLを維持・改善することである．
- 骨折危険因子として，わが国では低骨密度，脆弱性既存骨折，年齢があげられる．
- WHOのメタアナリシスでは過度のアルコール摂取（1日2単位以上），現在の喫煙，大腿骨近位部骨折の家族歴が確定している．
- 上記骨折危険因子を考慮した薬物治療開始基準が設定されている（図1）．
- 2006年版骨粗鬆症の予防と治療ガイドラインでは，国内外のエビデンスに基づき，骨密度，椎体骨折，非椎体骨折に対する薬剤効果を評価し，有害事象の発生リスクも含めた総合評価が行われている（表1）．
- 新しい治療薬として，ビスホスホネート製剤にミノドロネート，SERMにバゼドキシフェン製剤，そして骨形成促進薬としてテリパラチドが加わり治療の幅が格段に広がった．

治療計画を立てるまでに必要な情報と手順

症状・検査

①症状：骨粗鬆症にみられる主な臨床症候は，骨の脆弱化に起因する骨折と，その後の機能障害（QOL，ADLの低下）や慢性の疼痛である．この骨脆弱化は，骨の新陳代謝における骨吸収と骨形成のアンバランスにより発生する．すなわち，骨は常に骨吸収と骨形成により新陳代謝され新しい骨が形成されるが，その新陳代謝の場（basic multicellular unit；BMU，基礎的多細胞単位）においては若

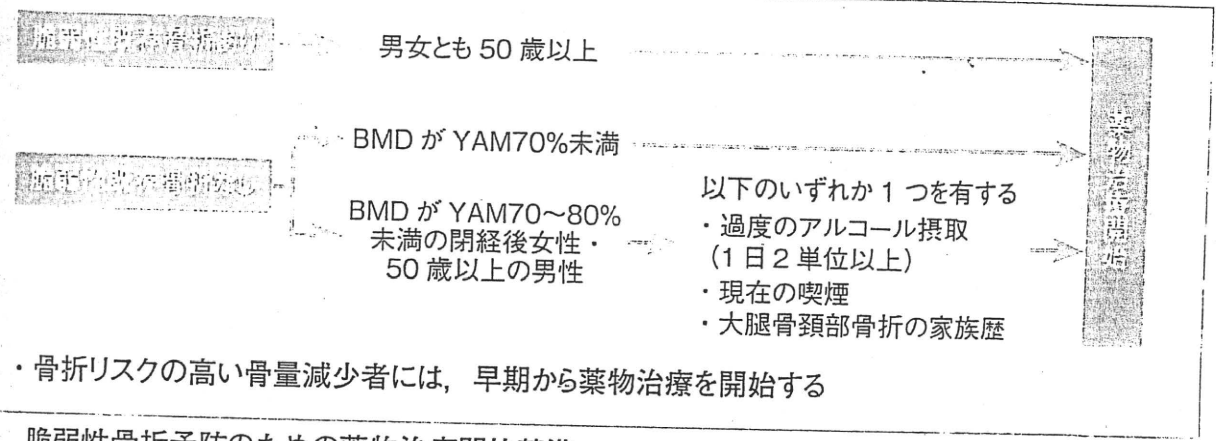

図1 脆弱性骨折予防のための薬物治療開始基準

（文献1）より引用）

nature medicine

Transcriptional regulation of endochondral ossification by HIF-2α during skeletal growth and osteoarthritis development

Taku Saito[1,2], Atsushi Fukai[1], Akihiko Mabuchi[3], Toshiyuki Ikeda[2], Fumiko Yano[4], Shinsuke Ohba[4], Nao Nishida[3], Toru Akune[5], Noriko Yoshimura[5], Takumi Nakagawa[1], Kozo Nakamura[1], Katsushi Tokunaga[3], Ung-il Chung[4] & Hiroshi Kawaguchi[1]

Chondrocyte hypertrophy followed by cartilage matrix degradation and vascular invasion, characterized by expression of type X collagen (COL10A1), matrix metalloproteinase-13 (MMP-13) and vascular endothelial growth factor (VEGF), respectively, are central steps of endochondral ossification during normal skeletal growth and osteoarthritis development. A *COL10A1* promoter assay identified hypoxia-inducible factor-2α (HIF-2α, encoded by *EPAS1*) as the most potent transactivator of *COL10A1*. HIF-2α enhanced promoter activities of *COL10A1*, *MMP13* and *VEGFA* through specific binding to the respective hypoxia-responsive elements. HIF-2α, independently of oxygen-dependent hydroxylation, was essential for endochondral ossification of cultured chondrocytes and embryonic skeletal growth in mice. HIF-2α expression was higher in osteoarthritic cartilages versus nondiseased cartilages of mice and humans. *Epas1*-heterozygous deficient mice showed resistance to osteoarthritis development, and a functional single nucleotide polymorphism (SNP) in the human *EPAS1* gene was associated with knee osteoarthritis in a Japanese population. The *EPAS1* promoter assay identified RELA, a nuclear factor-κB (NF-κB) family member, as a potent inducer of HIF-2α expression. Hence, HIF-2α is a central transactivator that targets several crucial genes for endochondral ossification and may represent a therapeutic target for osteoarthritis.

Endochondral ossification is an essential process not only for physiological skeletal growth[1], but also for development of osteoarthritis, which is the most common joint disorder and is characterized by cartilage degradation and osteophyte formation[2–7]. The process of endochondral ossification requires both the hypertrophic differentiation of chondrocytes, which is characterized by secretion of COL10A1, and the conversion of avascular cartilage tissue into highly vascularized bone tissue via degradation of the cartilage matrix and vascular invasion[1,8]. The matrix degradation requires proteinases, among which MMP-13 has a major role[8,9], and the vascular invasion depends on an angiogenic switch by VEGF[8,10]. These steps of chondrocyte hypertrophy, cartilage degradation and vascular invasion are well coordinated; however, the molecular mechanism that extensively controls the sequential steps remains an enigma. Here we initially performed a screen of transcription factors that potentiate the expression of *COL10A1* and identify HIF-2α, an α-subunit member of the HIF family, as the most potent transactivator.

The HIF protein family consists of α- and β-subunit members that function by forming heterodimers[11]. Under normoxic conditions, the α-subunit members HIF-1α, HIF-2α and HIF-3α undergo oxygen-dependent hydroxylation, resulting in ubiquitination and degradation by the proteasome[12,13]. In contrast, under hypoxic conditions, they are neither hydroxylated nor degraded, and they heterodimerize with the constitutive β-subunit members known as aryl hydrocarbon receptor nuclear translocator (ARNT), ARNT2, ARNT-like (ARNTL) and ARNTL2. The heterodimers activate transcription of the target genes by binding the consensus sequence called hypoxia-responsive element (HRE) in the promoters[11]. As cartilage is an avascular and hypoxic tissue, HIF proteins may have a crucial role in the functions of chondrocytes, and, in fact, HIF-1α is known be a potent regulator of cartilage homeostasis[14–16]. However, HIF-2α and HIF-1α are not functionally redundant[17–21], and little is known about the function of HIF-2α in chondrocytes. Here we examined the role of HIF-2α in endochondral ossification during skeletal growth and osteoarthritis development and investigate the underlying mechanism.

RESULTS

Identification of HIF-2α as a transactivator of *COL10A1*

We initially performed a screen of transcription factors that induce hypertrophic differentiation using mouse chondrogenic ATDC5 cells and human nonchondrogenic HeLa cells transfected with a proximal promoter fragment of the *COL10A1* gene. For candidate molecules, we

[1]Sensory & Motor System Medicine, University of Tokyo, Hongo, Bunkyo-ku, Tokyo, Japan. [2]Bone and Cartilage Regenerative Medicine, University of Tokyo, Hongo, Bunkyo-ku, Tokyo, Japan. [3]Human Genetics, University of Tokyo, Hongo, Bunkyo-ku, Tokyo, Japan. [4]Center for Disease Biology and Integrative Medicine, University of Tokyo, Hongo, Bunkyo-ku, Tokyo, Japan. [5]22nd Century Medical and Research Center, Faculty of Medicine, University of Tokyo, Hongo, Bunkyo-ku, Tokyo, Japan. Correspondence should be addressed to H.K. (kawaguchi-ort@h.u-tokyo.ac.jp).

Received 10 February; accepted 8 March; published online 23 May 2010; doi:10.1038/nm.2146

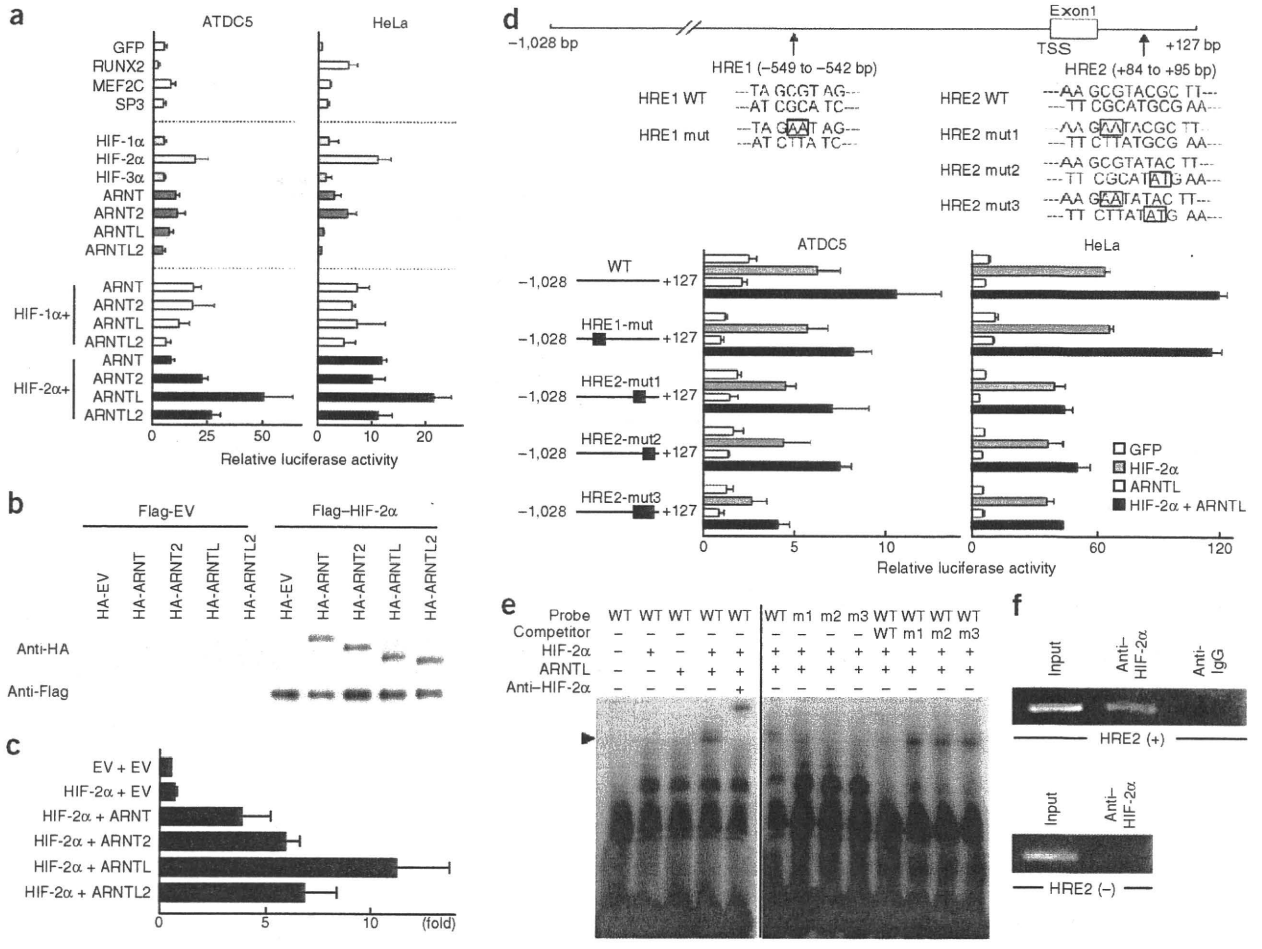

Figure 1 Transcriptional regulation of *COL10A1* by HIF-2α. (**a**) Luciferase assay for screening transcription factors that activate the *COL10A1* promoter by the transfections of candidate genes into ATDC5 and HeLa cells with a reporter construct containing a fragment (−1,028 to +127 bp) of the *COL10A1* gene. Data are shown as means ± s.d. (**b**) Immunoprecipitation and immunoblotting analysis by co-transfections of Flag-tagged HIF-2α or the control empty vector (EV) and hemagglutinin (HA)-tagged β-subunit members or the EV in ATDC5 cells. (**c**) Mammalian two-hybrid assay by transfections of vectors expressing GAL4–HIF-2α and VP16–β-subunit fusion proteins with the luciferase reporter vector with GAL4 binding sites into HeLa cells. Data are shown as means ± s.d. of relative fold increase in luciferase activity as compared to EV + EV (which is arbitrarily set to 1). (**d**) Site-directed mutagenesis analyses of the luciferase assay; one in HRE1 and three in HRE2 (+87 and +88 for mut1, +91 and +92 for mut2, and both for mut3), in the two cell lines transfected with GFP, HIF-2α, ARNTL or both HIF-2α and ARNTL. Data are shown as means ± s.d. (**e**) EMSA for specific binding (arrowhead) of the wild-type (WT) oligonucleotide probe containing HRE2 or the mutated probes described in **d** (m1, m2 and m3) with *in vitro*–translated HIF-2α, ARNT or both. Supershift by an antibody to HIF-2α (anti–HIF-2α) and cold competition with a 50-fold excess of unlabeled WT or the mutated probe are presented. (**f**) ChIP assay with cell lysates of human chondrogenic SW1353 cells that were amplified by a primer set spanning the HRE2 (+, +32 to +249 bp) or not spanning the HRE2 (−, −2,131 to −1,900 bp) before (input) and after immunoprecipitation with anti-HIF-2α or nonimmune IgG (anti-IgG).

prepared expression vectors of more than 100 transcription factors that are known to be expressed in chondrocytes, including HIF proteins, runt-related transcription factor-2 (RUNX2)[1,22], myocyte enhancer factor-2C (MEF2C)[23] and specificity protein-3 (SP3)[24] (**Fig. 1a**). Among them, HIF-2α showed the strongest activation in both cell lines. Although all β-subunit members were physically associated with HIF-2α in ATDC5 cells (**Fig. 1b**), ARNTL showed the strongest binding affinity to HIF-2α (**Fig. 1c**), and HIF-2α–ARNTL was the most potent combination for *COL10A1* transactivation (**Fig. 1a**).

In the *COL10A1* promoter, we identified two HREs by the consensus sequence [A/G]CGT (ref. 25), one in the 5′-end flanking region (HRE1) and the other in intron 1 (HRE2) (**Fig. 1d**). We introduced mutations in HRE1 and HRE2, but only the latter mutation resulted in suppression of transactivation by HIF-2α and the HIF-2α–ARNTL combination (**Fig. 1d**). We then confirmed the specific binding of the HIF-2α protein to HRE2 by electrophoretic mobility shift assay (EMSA) and chromatin immunoprecipitation (ChIP) assay (**Fig. 1e,f**).

HIF protein expression during chondrocyte differentiation

Although the HIF α- and β-subunit members were widely expressed in major tissues of adult mice, *Epas1* was most predominantly expressed in the tracheal cartilage (**Supplementary Fig. 1a**). During differentiation of ATDC5 cells, *Epas1* expression increased in accordance with the three representative factors for central steps of endochondral ossification: *Col10a1*, *Mmp13* and *Vegfa*, whereas *Hif1a* expression was strong at the early stage and decreased thereafter (**Fig. 2a**). *Hif3a* expression was very low, and the β-subunit members were extensively expressed in all differentiation stages (**Fig. 2a**).

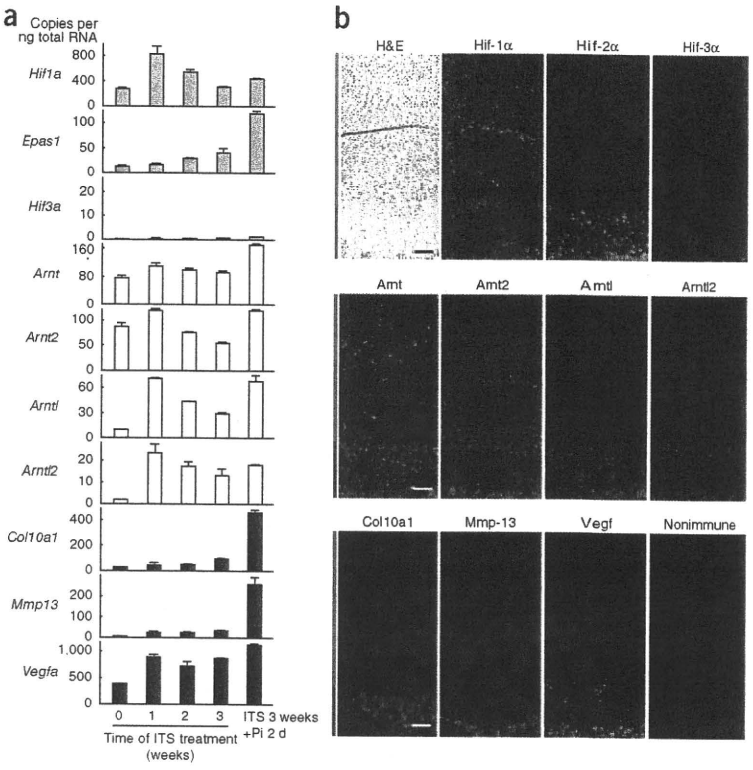

Figure 2 *In vitro* and *in vivo* expression patterns of the HIF α- and β-subunit members and Col10a1, Mmp-13 and Vegf during chondrocyte differentiation. (**a**) Time course of mRNA levels of the indicated genes during differentiation of mouse chondrogenic ATDC5 cells cultured with ITS (insulin, transferrin and sodium selenite) for 3 weeks and for 2 d more with inorganic phosphate (Pi). Data are expressed as means ± s.d. (**b**) H&E staining and immunofluorescence with antibodies to the indicated proteins, as well as a nonimmune control, in the proximal tibias of mouse embryos (embryonic day 18.5 (E18.5)). Scale bars, 100 μm. Red and blue bars to the left of each row indicate layers of proliferative and hypertrophic zones, respectively.

In tibial limb cartilage of mouse embryos, Hif-2α was localized primarily in the hypertrophic zone, similarly to Col10a1, Mmp-13 and Vegf (**Fig. 2b**). In contrast, Hif-1α was predominantly localized in chondrocytes at earlier differentiation stages in the proliferative zone, and Hif-3α was hardly detectable (**Fig. 2b**). The localizations of Arntl and Arntl2 were similar to Hif-2α, whereas those of Arnt and Arnt2 were similar to Hif-1α (**Fig. 2b**).

Physiological role of HIF-2α in endochondral ossification

To determine the involvement of HIF-2α in skeletal growth, we investigated the skeletal phenotype of *Epas1*-deficient mice. The homozygous deficient mutants (*Epas1*$^{-/-}$) were extraordinarily small and died at the early embryonic stage, as reported previously[20,21] (**Fig. 3a**). Although the heterozygous deficient mutants (*Epas1*$^{+/-}$) developed and grew without abnormalities of major organs, they showed mild but proportional dwarfism compared to wild-type littermates from embryonic stages up to 1 week after birth (**Fig. 3a,b** and **Supplementary Fig. 1b**). In the embryos, the limbs and vertebrae were 7–16% shorter in *Epas1*$^{+/-}$ mice than in the wild-type littermates (**Fig. 3c**). Although the actual length of the proliferative zone of the *Epas1*$^{+/-}$ limb was comparable to that of wild-type, the percentage of the proliferative zone relative to the total limb length was moderately increased (**Fig. 3d,e**) with normal BrdU-positive proliferative cells but suppressed Col10a1 expression (**Fig. 3f,g**), indicating impaired hypertrophic differentiation without an effect on proliferation caused by Hif-2α insufficiency. The percentage of the hypertrophic zone relative to the total limb length was also increased and that of the bone area was considerably decreased in the *Epas1*$^{+/-}$ limbs (**Fig. 3d,e**), indicating that Hif-2α insufficiency impaired not only chondrocyte hypertrophy but also subsequent steps such as matrix degradation and vascularization. This difference was gradually decreased with developmental compression of the hypertrophic zone after birth (**Supplementary Fig. 1c**). Immunohistochemistry confirmed that Mmp-13 and Vegf, as well as Col10a1, were suppressed by the Hif-2α insufficiency, which may cause the decrease in cartilage calcification shown by von Kossa staining (**Fig. 3f**).

Function of HIF-2α in cultured chondrocytes

In cultured ATDC5 cells, *Col10a1*, *Mmp13* and *Vegfa* amounts, as well as the activity of alkaline phosphatase and Alizarin red staining (both indicators of differentiation), were increased by overexpression of HIF-2α or the HIF-2α–ARNTL combination, whereas none of the expression levels or staining was affected by ARNTL alone (**Fig. 4a**). To examine the regulation of HIF-2α function by oxygen-dependent hydroxylation, we created ATDC5 lines overexpressing four kinds of HIF-2α mutants bearing mutations at the oxygen-dependent hydroxylation residues, including N847A and P531A (or both), which result in enhancement of the transactivation activity of the protein even under normoxic conditions, as well as P849A, which abrogates transactivation activity even under hypoxic conditions[13]. We found that none of these mutations affected the HIF-2α action on endochondral ossification parameters (**Fig. 4b**). All parameters were decreased, however, by loss of function of HIF-2α in ATDC5 cells achieved through overexpression of a dominant-negative mutant or expression of an siRNA specific for HIF-2α (**Fig. 4c**). In addition to ATDC cells, primary chondrocytes derived from *Epas1*$^{+/-}$ mice showed suppressed expression of the three factors, and the suppression of each factor was restored to wild-type levels by adenoviral overexpression of HIF-2α (**Fig. 4d**).

We then examined the transcriptional regulation of *MMP13* and *VEGFA* by HIF-2α. Among the α- and β-subunit members of the HIF proteins, HIF-2α most notably transactivated both *MMP13* and *VEGFA*, and the transactivation was further enhanced by ARNTL (**Supplementary Fig. 2a,b**), as is true for *COL10A1* (**Fig. 1a**). Deletion and site-directed mutagenesis analyses of the luciferase assay identified the core responsive elements to HIF-2α and the HIF-2α–ARNTL combination at HRE3 (−106 to −101) and HRE4 (−982 to −977) in the promoters of *MMP13* and *VEGFA*, respectively (**Supplementary Fig. 2c,d**). Further EMSA and ChIP assays confirmed the specific binding of the HIF-2α protein to HRE3 and HRE4 (**Supplementary Fig. 2e–h**).

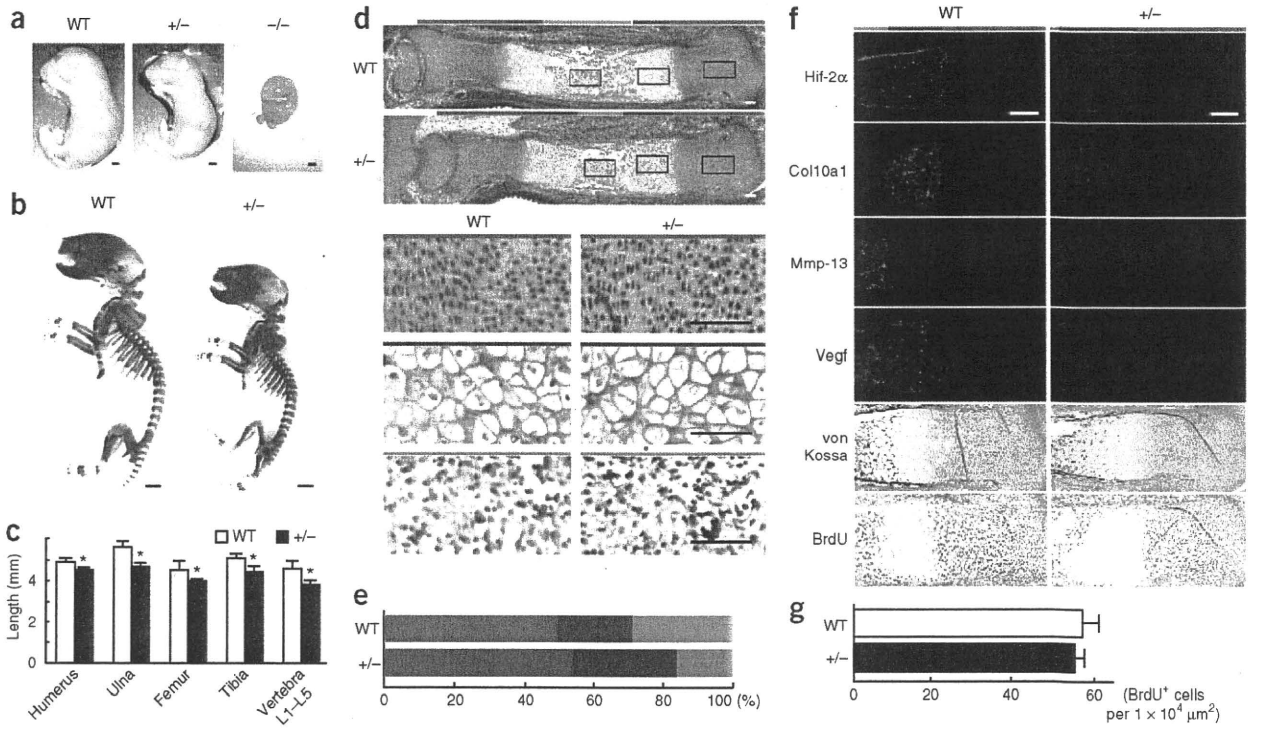

Figure 3 Skeletal abnormality in *Epas1*-deficient mice. (**a**) Wild-type (WT), heterozygous-deficient (*Epas1*$^{+/-}$) and homozygous-deficient (*Epas1*$^{-/-}$) littermate embryos (E17.5). All *Epas1*$^{-/-}$ embryos died at mid-gestation. Scale bars, 1 mm. (**b**) Double staining with Alizarin red and Alcian blue of the whole skeleton of WT and *Epas1*$^{+/-}$ littermate embryos (E17.5). Scale bars, 1 mm. (**c**) Length of long bones and vertebra (first to fifth lumbar spines) of WT and *Epas1*$^{+/-}$ littermate embryos. Data are expressed as means ± s.d. *$P < 0.05$ versus WT. (**d**) H&E staining of whole tibias of the WT and *Epas1*$^{+/-}$ littermate embryos. Inset boxes indicate the regions of the bottom three rows representing proliferative zone, hypertrophic zone and bone area, shown by red, blue and green bars, respectively. Scale bars, 100 μm. (**e**) Percentage of the length of proliferative zone (red), hypertrophic zone (blue) and bone area (green) over the total tibial length of the WT and *Epas1*$^{+/-}$ littermate embryos. (**f**) Immunofluorescence with antibodies to Hif-2α, Col10a1, Mmp-13 and Vegf, as well as bromodeoxyuridine (BrdU) labeling and von Kossa staining of the proximal tibias of WT and *Epas1*$^{+/-}$ littermate embryos (E17.5). Color bars indicate layers as indicated in **d**. Scale bars, 200 μm. (**g**) The number of BrdU-positive cells in 1×10^4 μm^2 of the proximal tibia of WT and *Epas1*$^{+/-}$ littermate embryos. Data are expressed as means ± s.d.

Contribution of HIF-2α to osteoarthritis in mice and humans

We next compared osteoarthritis development between adult littermates of wild-type and *Epas1*$^{+/-}$ mice that had undergone comparable skeletal growth after birth (**Supplementary Fig. 1b**) by creating a surgical osteoarthritis model through induction of instability to the knee joints[4,5]. The expression of Hif-2α, as well as of Col10a1, Mmp-13 and Vegf, increased in the joint cartilage with osteoarthritis development for 8 weeks after surgery in the wild-type mice; however, in the *Epas1*$^{+/-}$ littermates, the cartilage degradation and the expression of the three factors were notably suppressed (**Fig. 5a**). Quantification by grading systems[4,26] confirmed that the Hif-2α insufficiency caused significant resistance to cartilage degradation and osteophyte formation (**Fig. 5b**). There was no difference in the subchondral bones between the two genotypes under the sham operation, suggesting that the *Epas1* deficiency does not affect physiological bone homeostasis. However, after surgical induction, subchondral bone sclerosis, an osteoarthritic disorder secondary to cartilage destruction, was apparent in the wild-type joints, whereas it was suppressed in the *Epas1*$^{+/-}$ joints (**Supplementary Table 1**).

In human knee joint samples, as well, the HIF-2α expression increased with osteoarthritis development, reached a maximum at the initial and progressive stages and decreased thereafter at the terminal stage, although it was hardly detected in subchondral bone or synovium (**Fig. 5c**). To further investigate a possible association of the human *EPAS1* gene with knee osteoarthritis of humans, we searched a Japanese population-based cohort of the ROAD study[27] for sequence variations in exons and the 5′-end flanking region up to −1,000 bp from the transcription start site (TSS) of the human *EPAS1* gene and identified only one common SNP with a minor allele frequency >0.1, rs17039192 (+18C and +18T for major and minor alleles, respectively, relative to the TSS; minor allele frequency = 0.132) (**Fig. 5d**). A comparison of allelic frequencies between 397 individuals with knee osteoarthritis and 437 controls showed significant association of the rs17039192 SNP with knee osteoarthritis ($P = 0.013$, odds ratio = 1.44) (**Fig. 5d**). Because this SNP was located close to the TSS, we further examined the effects of the allelic difference (+18C/T) on *EPAS1* promoter activity in chondrogenic and nonchondrogenic cells transfected with a luciferase reporter gene and the *EPAS1* promoter fragment (−1,000 bp to 488 bp) containing +18C or +18T. The susceptibility allele (18C) showed higher promoter activity in chondrogenic cells, but not in nonchondrogenic cells (**Fig. 5e**), confirming that enhanced transactivation of *EPAS1* in chondrocytes is associated with osteoarthritis in humans.

Molecular network around HIF-2α in endochondral ossification

Regarding downstream molecules of HIF-2α, we have focused on COL10A1, MMP-13 and VEGF as representative factors for the

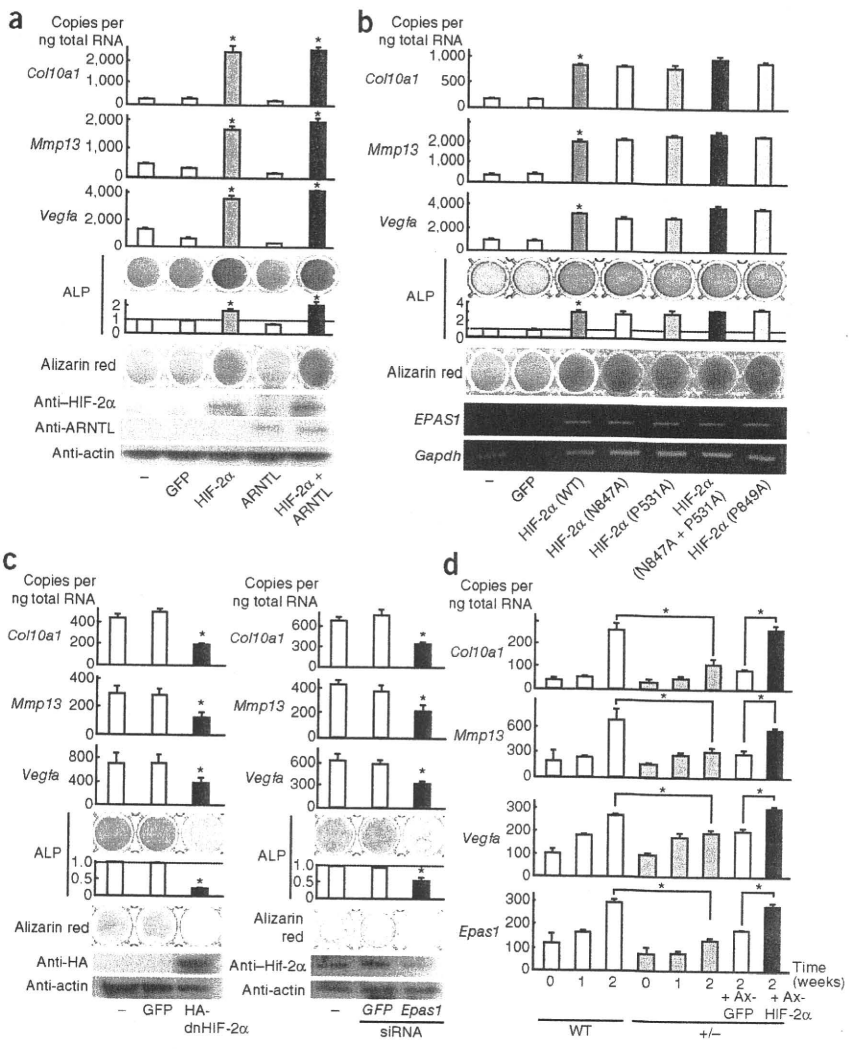

Figure 4 Effects of gain and loss of function of HIF-2α on endochondral ossification parameters in cultures of chondrogenic cells. (**a**) mRNA levels of *Col10a1*, *Mmp13* and *Vegfa*, alkaline phosphatase (ALP) activity (relative to control) and Alizarin red staining in stable lines of ATDC5 cells retrovirally transfected with GFP, HIF-2α, ARNTL or both HIF-2α and ARNTL and in nontransfected parental cells (–) after culture for 3 weeks with ITS and 2 d with Pi. HIF-2α and ARNTL levels were confirmed by western blotting, with the actin level as the internal control. (**b**) Analyses of the parameters in **a** in stable ATDC5 lines transfected with GFP or HIF-2α mutants at the oxygen-dependent hydroxylation residues causing enhancement (N847A and P531A) and abrogation (P849A) of HIF-2α transactivation activity under the culture conditions used in **a**. Gene expression was confirmed by RT-PCR with the *EPAS1* primer set inside the coding sequence, with the *Gapdh* level as the internal control. (**c**) Analyses of the same read-outs in **a** in stable ATDC5 lines transfected with GFP or HA-tagged dominant-negative HIF-2α (HA–dnHIF-2α) (left) or siRNA specific for *GFP* or *Epas1* mRNA (right) under the cultures conditions used in **a**. HA–dnHIF-2α and Hif-2α amounts were confirmed by western blotting. (**d**) mRNA levels of *Col10a1*, *Mmp13* and *Vegfa* and *Epas1* in the pellet cultures of primary chondrocytes derived from wild-type (WT) and *Epas1*$^{+/-}$ littermate embryos for 2 weeks. For the rescue experiment, adenoviral transfection with HIF-2α (Ax–HIF-2α) or the control GFP (Ax-GFP) was performed before the pellet formation. All data are expressed as means ± s.d. $^*P < 0.05$ versus GFP unless otherwise indicated.

central three steps of endochondral ossification (chondrocyte hypertrophy, cartilage degradation and vascularization) and found that all were the direct transcriptional targets. However, there are other factors related to endochondral ossification, including in the earlier cartilage formation step and in the later osteogenesis step, which might also be targets of HIF-2α. We therefore examined the expression patterns of the following factors: type II collagen (COL2A1) and aggrecan (AGC1) as cartilage matrix proteins; RUNX2, Indian hedgehog (IHH), and type 1 PTH/PTHrP receptor (PTH1R) as chondrocyte hypertrophy markers; MMP-3, MMP-9, a disintegrin and metalloproteinase with thrombospondin type 1 motif-4 (ADAMTS4) and ADAMTS5 as cartilage-degradable proteinases; and type I collagen (COL1A1), bone sialoprotein (BSP), osteocalcin, alkaline phosphatase, bone morphogenetic protein-2 (BMP-2), BMP-4 and BMP-7 as osteogenic markers. In cultured ATDC5 cells, expression of chondrocyte hypertrophy markers, cartilage degradable proteinases and osteogenic markers increased in accordance with the cell differentiation and *Epas1* expression (**Supplementary Fig. 3a**). The chondrocyte hypertrophy markers and cartilage degradable proteinases were localized mainly in the hypertrophic zone of the mouse limb cartilage, similarly to Hif-2α (**Supplementary Fig. 3b**). The mRNA levels of cartilage matrix proteins, chondrocyte hypertrophy markers and most of the osteogenic markers were increased in ATDC5 cells overexpressing HIF-2α or HIF-2α–ARNTL (**Supplementary Fig. 4a**). Among cartilage-degradable proteinases, expression of *Mmp3* and *Mmp9* was increased, whereas neither *Adamts4* nor *Adamts5* was affected (**Supplementary Fig. 4a**). In contrast, mRNA levels of the chondrocyte hypertrophy markers *Mmp3* and *Mmp9* were decreased after overexpression of a dominant-negative mutant form of HIF-2α and siRNA specific for *Epas1* mRNA in ATDC5 cells (**Supplementary Fig. 4b,c**); however, cartilage matrix proteins, *Adamts4*, *Adamts5* and most of osteogenic markers were little affected. Primary chondrocytes derived from *Epas1*$^{+/-}$ mice reproducibly showed suppression of the chondrocyte hypertrophy markers, *Mmp3* and *Mmp9*, but not cartilage matrix proteins, *Adamts4*, *Adamts5* or osteogenic factors, and the suppression was restored to wild-type levels by HIF-2α overexpression (**Supplementary Fig. 5**). Further *in vivo* analyses of embryonic limbs (**Supplementary Fig. 6a**) and osteoarthritic knee joints (**Supplementary Fig. 6b**) confirmed the decreases in expression of the chondrocyte hypertrophy markers, Mmp-3 and Mmp-9, but not cartilage matrix proteins Adamts4 or Adamts5, by Hif-2α insufficiency. HIF-2α enhanced the promoter activities of the chondrocyte hypertrophy markers *MMP3* and *MMP9*, as well as *Col10a1*, *Mmp13*, and *Vegfa* mRNA levels, much more strongly than HIF-1α, and the stimulation of the mRNA levels by HIF-2α was not altered by cotransfection of

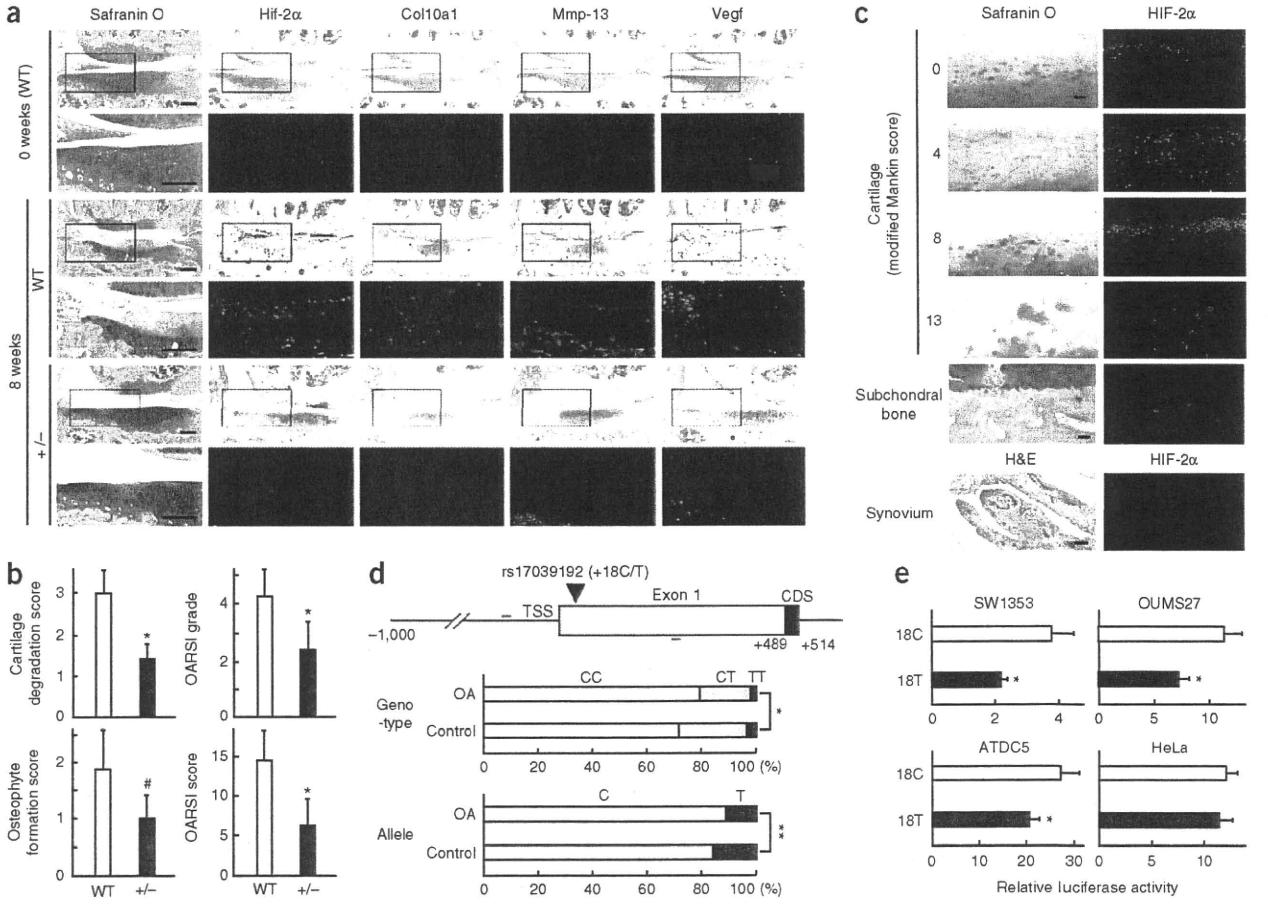

Figure 5 Contribution of HIF-2α to osteoarthritis development in mice and humans. (**a**) Cartilage degradation assessed by safranin O staining and expression of Hif-2α, Col10a1, Mmp-13 and Vegf by immunostaining (brown) and immunofluorescence (green) in mouse knee joints 0 and 8 weeks after creating a surgical osteoarthritis model in 8-week-old wild-type (WT) and *Epas1*$^{+/-}$ littermates. Boxed areas in each safranin O–stained or each immunostained image indicate the regions shown in the enlarged safranin O–stained or immunofluorescent image immediately below. Scale bars, 100 μm. (**b**) Quantification of osteoarthritis development by our (two left graphs) and OARSI (two right graphs) grading systems. Data are expressed as means ± s.d. #$P < 0.05$, *$P < 0.01$ versus WT. (**c**) Safranin O staining, H&E staining and immunofluorescence with an antibody to HIF-2α in human tibial cartilages of various degradation stages, subchondral bone (beneath the cartilage with Mankin score = 8) and synovium (around the cartilage with Mankin score = 8), obtained as surgical specimens of total knee arthroplasty. Scale bars, 100 μm. (**d**) Top, the identified SNP, rs17039192, and primers used for genotyping (red lines) in the human *EPAS1* gene. CDS, coding sequence. Bottom, association of the rs17039192 (+18C/T) SNP with knee osteoarthritis (OA) diagnosed on radiographs using the Kellgren/Lawrence grade in a Japanese population. The odds ratio of the susceptibility allele was 1.44 (95% confidence interval: 1.08–1.92). *$P = 0.05$, **$P = 0.013$. (**e**) Luciferase activities in chondrogenic SW1353, OUMS27 and ATDC5 cells and nonchondrogenic HeLa cells transfected with a luciferase reporter gene construct ligated to a fragment (−1,000 bp to +488 bp) containing +18C or +18T. Data are shown as means ± s.d. *$P < 0.05$ versus 18C.

HIF-1α (**Supplementary Fig. 7a,b**). Furthermore, the endochondral ossification parameters stimulated by HIF-2α overexpression in ATDC5 cells were not inhibited by suppression of RUNX2 through overexpression of a dominant-negative mutant RUNX2 (**Supplementary Fig. 7c**).

Finally, to identify the upstream mechanism that regulates HIF-2α, we performed a screen of transcription factors with the *EPAS1* promoter fragment including the +18C SNP described above. Among candidate molecules that are known to regulate chondrocyte differentiation, such as sex-determining region Y box (SOX), RUNX, CCAAT/enhancer binding protein (C/EBP), MEF2, SP/Kruppel-like factor (KLF), activating transcription factor (ATF), cAMP responsive element–binding protein (CREB), Notch and NF-κB family members, we found that v-rel reticuloendotheliosis viral oncogene homolog A (RELA or NF-κB p65), an essential molecule of the NF-κB signal, showed the strongest activation in all cells (**Fig. 6a**). In the *EPAS1* promoter we identified an NF-κB motif and found that site-directed mutagenesis in the motif caused suppression of transactivation by RELA (**Fig. 6b**). The allelic difference (+18C/T) of the rs17039192 SNP described above also altered the activation of *EPAS1* promoter by RELA but did not affect it when the NF-κB motif was mutated, suggesting the involvement of this SNP in the *EPAS1* transactivation and osteoarthritis development caused by the NF-κB signal. We further confirmed that the proinflammatory cytokines tumor necrosis factor-α (TNF-α) and interleukin-1β (IL-1β), putative inducers of the NF-κB signal[28], increased *EPAS1* expression in cultured chondrogenic cells (**Fig. 6c**). In mouse knee joint cartilage, the expression of Rela was increased during osteoarthritis development, similarly to Hif-2α expression (**Fig. 6d**).

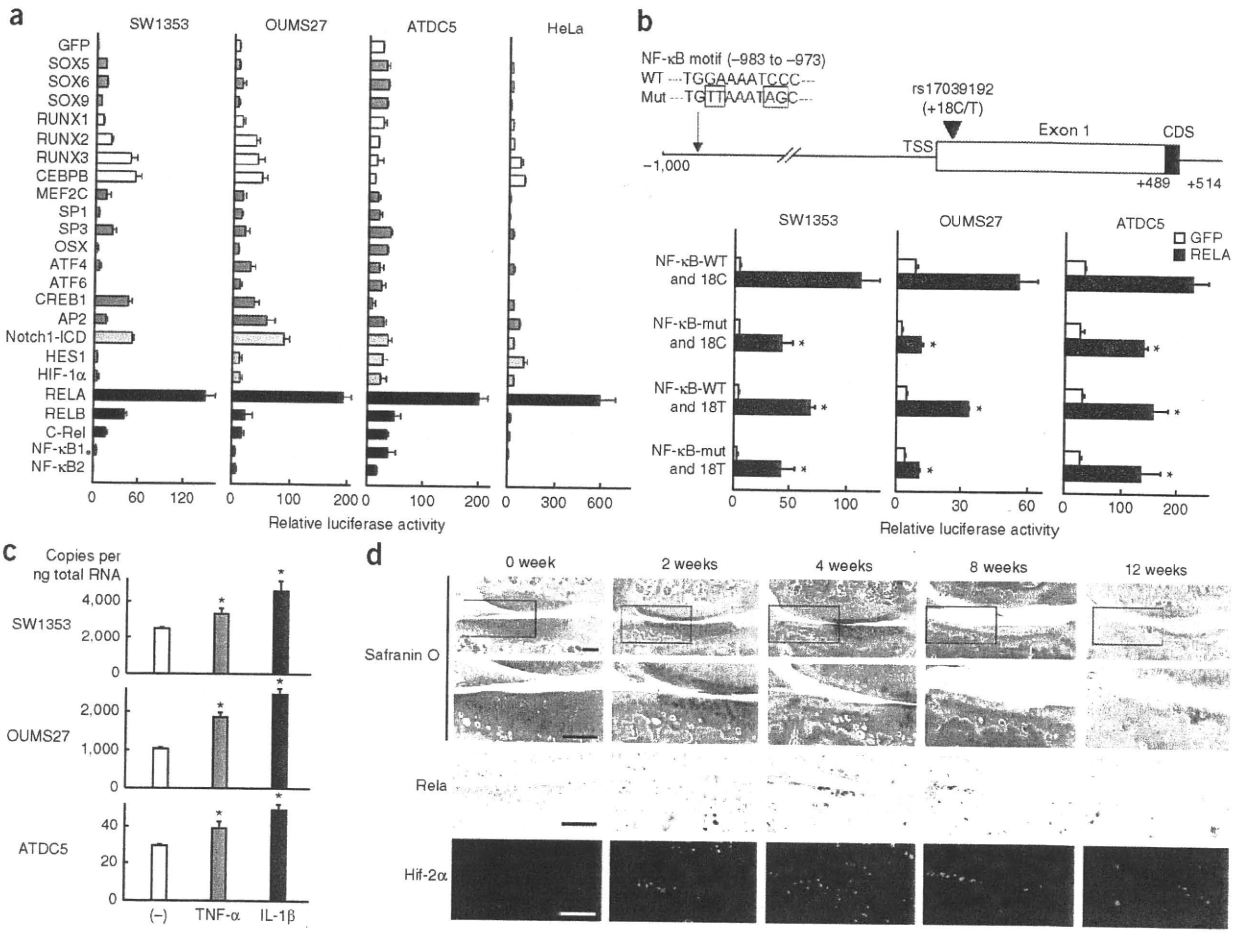

Figure 6 Upstream mechanism that regulates HIF-2α. (**a**) Luciferase activities after transfections of putative chondrocyte-related transcription factors into chondrogenic SW1353, OUMS27 and ATDC5 cells and nonchondrogenic HeLa cells with a reporter construct containing a fragment (–1,000 bp to +488 bp) of the *EPAS1* gene. OSX, osterix; AP2, transcription factor AP-2α; Notch1-ICD, intercellular domain of Notch1; HES1, hairy and enhancer of split 1. Data are shown as means ± s.d. (**b**) Top, depiction of the NF-κB motif (–983 to –973) in the human *EPAS1* gene. Bottom, site-directed mutagenesis analyses of the luciferase assay in the three chondrogenic cell lines transfected with GFP or RELA. Luciferase activities were compared with or without mutation in the NF-κB motif and with +18C or +18T of the rs17039192 SNP. Data are shown as means ± s.d. $^*P < 0.05$ versus wild-type NF-κB and 18C with RELA. (**c**) mRNA levels of *EPAS1* in the three chondrogenic cells cultured with or without TNF-α or IL-1β (each 1 ng ml^{-1}) for 2 d. Data are expressed as means ± s.d. $^*P < 0.05$ versus control. (**d**) Time course of degradation in mouse knee joint cartilage, as shown by Safranin O staining and expression of Rela and Hif-2α by immunostaining and immunofluorescence, respectively, in a surgical osteoarthritis model in 8-week-old mice. Boxed areas in each of the top images are enlarged in the bottom images directly beneath. Scale bar, 100 μm.

DISCUSSION

Among the sequential steps of endochondral ossification—cartilage formation, chondrocyte hypertrophy, cartilage degradation, vascularization and osteogenesis—this study reveals that HIF-2α functions as an extensive transcriptional regulator of the central three steps. HIF-2α shares about 50% amino acid homology with HIF-1α (ref. 20), a potent regulator of cartilage homeostasis[14–16]; however, accumulating evidence has shown distinct expression patterns and functions between the two HIF proteins[17–21]. HIF-1α is expressed mainly in hypovascular and hypoxic tissues[16,19,29], whereas HIF-2α is expressed even in vascularized tissues[11,29]. In cartilage as well, previous studies and our current study show that HIF-1α is expressed from the early stage of cartilage formation, and its activity is enhanced by hypoxia[13–16,30]. In contrast, HIF-2α is expressed mainly in highly differentiated chondrocytes, and its function is independent of oxygen-dependent hydroxylation. Likewise, although cartilage-specific knockout of HIF-1α leads to defects in the earlier stage of cartilage formation and the later stage of chondrocyte survival and osteogenesis[14–16], *Epas1*$^{+/-}$ mice show growth retardation with defects in the central steps of endochondral ossification. Hence, HIF-1α and HIF-2α may have distinct roles via different mechanisms: hypoxia-dependent cartilage formation and maintenance by HIF-1α and less hypoxia-dependent endochondral ossification by HIF-2α. We have also confirmed that neither gain nor loss of function of HIF-2α alters HIF-1α expression during chondrocyte differentiation, nor does HIF-1α transfection affect *EPAS1* promoter activity. Furthermore, HIF-1α hardly stimulates the expression of markers of the central steps of endochondral ossification in the presence or absence of HIF-2α, indicating independent functions of HIF-1α and HIF-2α at least in the central steps. However, we do not deny the possibility of interactions between HIF-1α and HIF-2α in earlier and later stages of endochondral ossification. The HIF-2α function may possibly be compensated by HIF-1α in this earlier stage, as cartilage matrix proteins are not altered by HIF-2α suppression. In the later or severe stage of osteoarthritic

cartilage, expression of HIF-2α decreases after reaching a maximum at the initiation of cartilage degradation in mice and humans, as was reported in a previous study[31]. In this terminal stage, the decreased HIF-2α expression may enhance autophagy in mature chondrocytes of osteoarthritic cartilage, as HIF-2α is known to antagonize the autophagy-accelerator function of HIF-1α[32].

Our study reveals that *COL10A1*, *MMP13* and *VEGFA* are the direct transcriptional targets of HIF-2α. The functional relationships *in vivo* are supported by previous reports that a deficiency of *Mmp13* or *Vegfa* in mice causes a skeletal phenotype similar to that in *Epas1*$^{+/-}$ mice, with elongation of the hypertrophic zone and delay of ossification in the limb cartilage[9,10], although the skeletal phenotypes of *Col10a1*-knockout mice differs among the reports[33–35]. Our further studies identify *RUNX2*, *IHH*, *PTH1R*, *MMP3* and *MMP9* as possible transcriptional targets of HIF-2α. We have recently reported that HIF-2α enhances *Runx2* promoter activity[36] and that *Runx2*$^{+/-}$ mice show resistance to osteoarthritis development under mechanical instability, similarly to *Epas1*$^{+/-}$ mice[5]. However, HIF-2α and RUNX2 may promote endochondral ossification via independent mechanisms.

There are two mechanisms of osteoarthritis protection: induction of anabolism or inhibition of catabolism in joint cartilage. The protection in *Epas1*$^{+/-}$ mice is not likely to be due to induction of anabolism, as the anabolic markers COL2A1 and AGC1 are unaffected in joint cartilage. Although recent studies have identified ADAMTS5 and related molecules as key catabolic regulators of osteoarthritis development[37–40], neither ADAMTS4 nor ADAMTS5 is regulated by HIF-2α, implicating another pathway. Because *Mmp13*$^{-/-}$ mice are reported to be protected from cartilage degradation despite considerable aggrecan loss after surgical osteoarthritis induction[41], similarly to *Epas1*$^{+/-}$ mice, the osteoarthritis protection caused by the Hif-2α insufficiency might occur principally through regulation of Mmp-13.

Suppression of osteoarthritis development was obvious in *Epas1*$^{+/-}$ mice, whereas skeletal growth retardation was mild and transient, suggesting that pathological endochondral ossification is more dependent on HIF-2α than is physiological endochondral ossification. As a trigger of osteoarthritis, mechanical stress may induce the upstream NF-κB signal and HIF-2α expression in joint cartilage, which causes endochondral ossification by transactivation of *COL10A1*, *MMP13*, *VEGFA* and other factors. Recent comprehensive profiling analyses of not only genes and proteins, but also microRNAs, is unraveling the molecular network underlying osteoarthtitis development[42]; however, we hereby propose that signals in the HIF-2α axis from NF-κB signaling to endochondral ossification–related molecules may represent a rational therapeutic target for osteoarthritis with minimal effects on physiological skeletal homeostasis.

METHODS

Methods and any associated references are available in the online version of the paper at http://www.nature.com/naturemedicine/.

Note: Supplementary information is available on the Nature Medicine website.

ACKNOWLEDGMENTS

We thank R. Yamaguchi and H. Kawahara for technical assistance. This study was supported by a grant-in-aid for Scientific Research from the Japanese Ministry of Education, Culture, Sports, Science and Technology (19109007 and 20689028). The sponsor had no role in study design, data collection, data analysis, data interpretation or writing of the manuscript.

AUTHOR CONTRIBUTIONS

T.S., T.I. and H.K. performed project planning; T.S., A.F., A.M., F.Y. and S.O. performed the experiments; T.S., A.M., N.N., T.A., N.Y., T.N., K.N., K.T., U.-i.C. and H.K. conducted data analysis; T.S. and H.K. wrote the manuscript.

COMPETING FINANCIAL INTERESTS

The authors declare no competing financial interests.

Published online at http://www.nature.com/naturemedicine/.
Reprints and permissions information is available online at http://npg.nature.com/reprintsandpermissions/.

1. Kronenberg, H.M. Developmental regulation of the growth plate. *Nature* **423**, 332–336 (2003).
2. Kühn, K., D'Lima, D.D., Hashimoto, S. & Lotz, M. Cell death in cartilage. *Osteoarthritis Cartilage* **12**, 1–16 (2004).
3. Kawaguchi, H. Endochondral ossification signals in cartilage degradation during osteoarthritis progression in experimental mouse models. *Mol. Cells* **25**, 1–6 (2008).
4. Kamekura, S. *et al.* Osteoarthritis development in novel experimental mouse models induced by knee joint instability. *Osteoarthritis Cartilage* **13**, 632–641 (2005).
5. Kamekura, S. *et al.* Contribution of runt-related transcription factor 2 to the pathogenesis of osteoarthritis in mice after induction of knee joint instability. *Arthritis Rheum.* **54**, 2462–2470 (2006).
6. Yamada, T. *et al.* Carminerin contributes to chondrocyte calcification during endochondral ossification. *Nat. Med.* **12**, 665–670 (2006).
7. Drissi, H., Zuscik, M., Rosier, R. & O'Keefe, R. Transcriptional regulation of chondrocyte maturation: potential involvement of transcription factors in OA pathogenesis. *Mol. Aspects Med.* **26**, 169–179 (2005).
8. Ortega, N., Behonick, D.J. & Werb, Z. Matrix remodeling during endochondral ossification. *Trends Cell Biol.* **14**, 86–93 (2004).
9. Stickens, D. *et al.* Altered endochondral bone development in matrix metalloproteinase 13–deficient mice. *Development* **131**, 5883–5895 (2004).
10. Zelzer, E. *et al.* VEGFA is necessary for chondrocyte survival during bone development. *Development* **131**, 2161–2171 (2004).
11. Semenza, G.L. HIF-1 and human disease: one highly involved factor. *Genes Dev.* **14**, 1983–1991 (2000).
12. Schofield, C.J. & Ratcliffe, P.J. Oxygen sensing by HIF hydroxylases. *Nat. Rev. Mol. Cell Biol.* **5**, 343–354 (2004).
13. Lando, D., Peet, D.J., Whelan, D.A., Gorman, J.J. & Whitelaw, M.L. Asparagine hydroxylation of the HIF transactivation domain a hypoxic switch. *Science* **295**, 858–861 (2002).
14. Pfander, D., Cramer, T., Schipani, E. & Johnson, R.S. HIF-1α controls extracellular matrix synthesis by epiphyseal chondrocytes. *J. Cell Sci.* **116**, 1819–1826 (2003).
15. Schipani, E. Hypoxia and HIF-1α in chondrogenesis. *Ann. NY Acad. Sci.* **1068**, 66–73 (2006).
16. Schipani, E. *et al.* Hypoxia in cartilage: HIF-1α is essential for chondrocyte growth arrest and survival. *Genes Dev.* **15**, 2865–2876 (2001).
17. Patel, S.A. & Simon, M.C. Biology of hypoxia-inducible factor-2α in development and disease. *Cell Death Differ.* **15**, 628–634 (2008).
18. O'Rourke, J.F., Tian, Y.M., Ratcliffe, P.J. & Pugh, C.W. Oxygen-regulated and transactivating domains in endothelial PAS protein 1: comparison with hypoxia-inducible factor-1α. *J. Biol. Chem.* **274**, 2060–2071 (1999).
19. Jain, S., Maltepe, E., Lu, M.M., Simon, C. & Bradfield, C.A. Expression of ARNT, ARNT2, HIF1 α, HIF2 α and Ah receptor mRNAs in the developing mouse. *Mech. Dev.* **73**, 117–123 (1998).
20. Tian, H., Hammer, R.E., Matsumoto, A.M., Russell, D.W. & McKnight, S.L. The hypoxia-responsive transcription factor EPAS1 is essential for catecholamine homeostasis and protection against heart failure during embryonic development. *Genes Dev.* **12**, 3320–3324 (1998).
21. Scortegagna, M. *et al.* Multiple organ pathology, metabolic abnormalities and impaired homeostasis of reactive oxygen species in *Epas1*$^{-/-}$ mice. *Nat. Genet.* **35**, 331–340 (2003).
22. Komori, T. Regulation of skeletal development by the Runx family of transcription factors. *J. Cell. Biochem.* **95**, 445–453 (2005).
23. Arnold, M.A. *et al.* MEF2C transcription factor controls chondrocyte hypertrophy and bone development. *Dev. Cell* **12**, 377–389 (2007).
24. Magee, C., Nurminskaya, M., Faverman, L., Galera, P. & Linsenmayer, T.F. SP3/SP1 transcription activity regulates specific expression of collagen type X in hypertrophic chondrocytes. *J. Biol. Chem.* **280**, 25331–25338 (2005).
25. Pescador, N. *et al.* Identification of a functional hypoxia-responsive element that regulates the expression of the egl nine homologue 3 (egln3/phd3) gene. *Biochem. J.* **390**, 189–197 (2005).
26. Pritzker, K.P. *et al.* Osteoarthritis cartilage histopathology: grading and staging. *Osteoarthritis Cartilage* **14**, 13–29 (2006).
27. Muraki, S. *et al.* Prevalence of radiographic knee osteoarthritis and its association with knee pain in the elderly of Japanese population-based cohorts: the ROAD study. *Osteoarthritis Cartilage* **17**, 1137–1143 (2009).
28. Li, Q. & Verma, I.M. NF-κB regulation in the immune system. *Nat. Rev. Immunol.* **2**, 725–734 (2002).
29. Stewart, A.J., Houston, B. & Farquharson, C. Elevated expression of hypoxia inducible factor-2α in terminally differentiating growth plate chondrocytes. *J. Cell. Physiol.* **206**, 435–440 (2006).
30. Amarilio, R. *et al.* HIF1α regulation of Sox9 is necessary to maintain differentiation of hypoxic prechondrogenic cells during early skeletogenesis. *Development* **134**, 3917–3928 (2007).

31. Bohensky, J. *et al.* Regulation of autophagy in human and murine cartilage: hypoxia-inducible factor 2 suppresses chondrocyte autophagy. *Arthritis Rheum.* **60**, 1406–1415 (2009).
32. Srinivas, V., Bohensky, J., Zahm, A.M. & Shapiro, I.M. Autophagy in mineralizing tissues: microenvironmental perspectives. *Cell Cycle* **8**, 391–393 (2009).
33. Gress, C.J. & Jacenko, O. Growth plate compressions and altered hematopoiesis in collagen X null mice. *J. Cell Biol.* **149**, 983–993 (2000).
34. Kwan, K.M. *et al.* Abnormal compartmentalization of cartilage matrix components in mice lacking collagen X: implications for function. *J. Cell Biol.* **136**, 459–471 (1997).
35. Rosati, R. *et al.* Normal long bone growth and development in type X collagen–null mice. *Nat. Genet.* **8**, 129–135 (1994).
36. Tamiya, H. *et al.* Analysis of the Runx2 promoter in osseous and non-osseous cells and identification of HIF2A as a potent transcription activator. *Gene* **416**, 53–60 (2008).
37. Echtermeyer, F. *et al.* Syndecan-4 regulates ADAMTS-5 activation and cartilage breakdown in osteoarthritis. *Nat. Med.* **15**, 1072–1076 (2009).
38. Glasson, S.S. *et al.* Deletion of active ADAMTS5 prevents cartilage degradation in a murine model of osteoarthritis. *Nature* **434**, 644–648 (2005).
39. Lin, A.C. *et al.* Modulating hedgehog signaling can attenuate the severity of osteoarthritis. *Nat. Med.* **15**, 1421–1425 (2009).
40. Stanton, H. *et al.* ADAMTS5 is the major aggrecanase in mouse cartilage in vivo and in vitro. *Nature* **434**, 648–652 (2005).
41. Little, C.B. *et al.* Matrix metalloproteinase 13-deficient mice are resistant to osteoarthritic cartilage erosion but not chondrocyte hypertrophy or osteophyte development. *Arthritis Rheum.* **60**, 3723–3733 (2009).
42. Iliopoulos, D., Malizos, K.N., Oikonomou, P. & Tsezou, A. Integrative microRNA and proteomic approaches identify novel osteoarthritis genes and their collaborative metabolic and inflammatory networks. *PLoS One* **3**, e3740 (2008).

ONLINE METHODS

Cell cultures. We cultured HeLa (Riken BRC), OUMS27 (the Health Science Research Resources Bank) and SW1353 (American Type Culture Collection) cells in DMEM with 10% FBS and ATDC5 cells (Riken BRC) in DMEM and F12 (1:1) with 5% FBS, and we performed experiments using these cell lines as previously described[43]. We used TNF-α and IL-1β (Peprotech) at final concentrations of 1 ng ml^{-1} for 2 d.

Construction of expression vectors. We prepared expression vectors for the luciferase assay and for co-immunoprecipitation in pCMV-HA (Clontech) and pCMV-3Tag-1A (Stratagene), respectively, and created the dnRUNX2, dnHIF-2α and HIF-2α mutants at the oxygen-dependent hydroxylation residues as previously described[13,44,45]. We constructed an siRNA vector for the mouse *Epas1* gene (nucleotides 1,140–1,160) with piGENEmU6 vector (iGENE Therapeutics)[46] and pMx vectors[47], retrovirus vectors using pMx vectors[47,48], adenovirus vectors by the AdenoX Expression system (Clontech), and we verified all vectors by DNA sequencing.

Luciferase assay. We prepared the *COL10A1* promoter region (from −1,028 to +127 bp relative to the TSS), *MMP13* (−1,000 to 0), *VEGFA* (−1,000 to 0), *RUNX2* (−1,480 to 0), *IHH* (−1,488 to 0), *PTH1R* (−1,529 to 0), *MMP3* (−1,551 to +39), *MMP9* (−1,775 to +17) and *EPAS1* (−1,000 to +488) by PCR using human genomic DNA as the template, and we cloned them into the pGL3-Basic vector or the pGL4.10[luc2] vector (Promega). We created deletion and mutation constructs by PCR, performed luciferase assays with the Dual-Luciferase Reporter Assay System (Promega) and showed the data as the ratio of the firefly activities to the *Renilla* activities.

Co-immunoprecipitation and mammalian two-hybrid assays. We performed co-immunoprecipitation with EZ view Red Protein A and anti-FLAG M2 Affinity Gels (Sigma) and mammalian two-hybrid assays with the Checkmate mammalian two-hybrid system (Promega).

Electrophoretic mobility shift assay. We prepared HIF-2α and ARNTL proteins by *in vitro* translation with the TNT T7 Quick System (Promega) and the pCITE4 vector (Novagen), and we performed the EMSA with the DIG Gel Shift Kit (Roche). Regions of the oligonucleotide probe were as follows: *COL10A1*, from +70 to +111 bp relative to the TSS; *MMP13*, −125 to −81; *VEGFA*, −1,002 to −957.

Chromatin immunoprecipitation assay. We performed the ChIP assay in SW1353 cells with a OneDay ChIP kit (Diagenode). For immunoprecipitation, we used antibodies to HIF-2α (Santa Cruz Biotechnology) and the normal rabbit IgG (Invitrogen). Primer sets, one spanning and the other not spanning the identified enhancer element, are as follows: *COL10A1*, +32 to +249 and −2,131 to −1,900; *MMP13*, −214 to −29 and −4,797 to −4,551; *VEGFA*, −1,000 to −795 and −4,685 to −4,507, respectively.

Mice. We purchased Hif-2α-mutant mice[20] from the Jackson Laboratory. In each experiment, we compared male *Epas1*$^{+/-}$ and wild-type littermates. We performed all experiments according to a protocol approved by the Animal Care and Use Committee of the University of Tokyo. We isolated primary chondrocytes from the ribs of mouse embryos, cultured them in a monolayer for 2 d and in a pellet for additional 2 weeks in DMEM with 10% FBS and transduced adenoviruses at 100 multiplicities of infection 4 h before the pellet formation.

Osteoarthritis experiment. We performed the surgical procedure to create an experimental osteoarthritis model on 8-week-old male mice as previously reported[4–6], and we analyzed them 8 weeks after surgery. We quantified osteoarthritis severity by our original grading system[4] and by the OARSI system (0–6 for grade and 0–24 for score)[26], which was assessed by a single observer who was blinded to the experimental group. We performed histomorphometric measurements in eight optical fields of the subchondral bones, according to the American Society for Bone and Mineral Research nomenclature report[49].

Human samples. We obtained human samples from individuals undergoing total knee arthroplasty after obtaining written informed consent as approved by the Ethics Committee of the University of Tokyo. We histologically assessed cartilage samples with the modified Mankin scoring system[50,51].

Case-control association study. We recruited individuals over 50 years of age with (n = 397; mean age, 75.6; range, 53–89) and without (n = 437; mean age, 73.6; range, 60–87) knee osteoarthritis in a population-based cohort of the ROAD study[27]. We diagnosed osteoarthritis on the basis of radiographic findings by the Kellgren-Lawrence grading system[52]: the knee osteoarthritis population included individuals with grades 3 and 4 and the control population with grades 0 and 1. After obtaining written informed consent as approved by the Ethics Committee of the University of Tokyo, we extracted genomic DNA from peripheral blood leukocytes of individuals using standard protocols. We searched SNPs around the *EPAS1* gene using the dbSNP database, and we genotyped the identified SNP by PCR restriction fragment length polymorphism (RFLP) using BanI as the enzyme. We confirmed that the P value of the Hardy-Weinberg equilibrium test in the control population was higher than 0.01.

Other analyses. We performed real-time RT-PCR, western blotting and histological analyses as previously reported[48,53]. Primer sequences and antibody information are available upon request.

Statistical analyses. We performed statistical analyses of experimental data with the unpaired two-tailed Student's t test. In the case control association study, we evaluated genotypic and allelic models by the χ^2 test for the Hardy-Weinberg equilibrium using spreadsheet software (Excel). P values less than 0.05 were considered significant.

43. Saito, T., Ikeda, T., Nakamura, K., Chung, U.I. & Kawaguchi, H. S100A1 and S100B, transcriptional targets of SOX trio, inhibit terminal differentiation of chondrocytes. *EMBO Rep.* **8**, 504–509 (2007).
44. Maemura, K. *et al.* Generation of a dominant-negative mutant of endothelial PAS domain protein 1 by deletion of a potent C-terminal transactivation domain. *J. Biol. Chem.* **274**, 31565–31570 (1999).
45. Ueta, C. *et al.* Skeletal malformations caused by overexpression of Cbfa1 or its dominant negative form in chondrocytes. *J. Cell Biol.* **153**, 87–100 (2001).
46. Miyagishi, M. & Taira, K. RNAi expression vectors in mammalian cells. *Methods Mol. Biol.* **252**, 483–491 (2004).
47. Kitamura, T. New experimental approaches in retrovirus-mediated expression screening. *Int. J. Hematol.* **67**, 351–359 (1998).
48. Morita, S., Kojima, T. & Kitamura, T. Plat-E: an efficient and stable system for transient packaging of retroviruses. *Gene Ther.* **7**, 1063–1066 (2000).
49. Parfitt, A.M. *et al.* Bone histomorphometry: standardization of nomenclature, symbols, and units. Report of the ASBMR Histomorphometry Nomenclature Committee. *J. Bone Miner. Res.* **2**, 595–610 (1987).
50. Mankin, H.J., Dorfman, H., Lippiello, L. & Zarins, A. Biochemical and metabolic abnormalities in articular cartilage from osteo-arthritic human hips. II. Correlation of morphology with biochemical and metabolic data. *J. Bone Joint Surg. Am.* **53**, 523–537 (1971).
51. Ostergaard, K., Andersen, C.B., Petersen, J., Bendtzen, K. & Salter, D.M. Validity of histopathological grading of articular cartilage from osteoarthritic knee joints. *Ann. Rheum. Dis.* **58**, 208–213 (1999).
52. Kellgren, J.H. & Lawrence, J.S. Radiological assessment of osteo-arthrosis. *Ann. Rheum. Dis.* **16**, 494–502 (1957).
53. Hirata, M. *et al.* C/EBPβ promotes transition from proliferation to hypertrophic differentiation of chondrocytes through transactivation of p57. *PLoS One* **4**, e4543 (2009).

Osteoarthritis and Cartilage 18 (2010) 1227–1234

Osteoarthritis and Cartilage

Association of radiographic and symptomatic knee osteoarthritis with health-related quality of life in a population-based cohort study in Japan: the ROAD study

S. Muraki †*, T. Akune †, H. Oka ‡, Y. En-yo §, M. Yoshida §, A. Saika §, T. Suzuki ||, H. Yoshida ||, H. Ishibashi ||, F. Tokimura ||, S. Yamamoto ||, K. Nakamura ¶, H. Kawaguchi ¶, N. Yoshimura ‡

† *Department of Clinical Motor System Medicine, 22nd Century Medical and Research Center, Faculty of Medicine, The University of Tokyo, Tokyo, Japan*
‡ *Department of Joint Disease Research, 22nd Century Medical and Research Center, Faculty of Medicine, The University of Tokyo, Tokyo, Japan*
§ *Department of Orthopaedic Surgery, Wakayama Medical University, Wakayama, Japan*
|| *Tokyo Metropolitan Institute of Gerontology, Tokyo, Japan*
¶ *Department of Sensory & Motor System Medicine, Faculty of Medicine, The University of Tokyo, Tokyo, Japan*

ARTICLE INFO

Article history:
Received 4 August 2009
Accepted 17 June 2010

Keywords:
Osteoarthritis
Knee
Quality of life
Cohort
Epidemiology

SUMMARY

Objective: Knee osteoarthritis (OA) is a major public health issue causing chronic pain and disability. However, there is little information on the impact of this disease on quality of life (QOL) in Japanese men and women. The objective of the present study was to clarify the impact of radiographic and symptomatic knee OA on QOL in Japan.

Methods: This study examined the association of radiographic and symptomatic knee OA with QOL parameters such as the Medical Outcomes Study Short Form-8 (SF-8), EuroQOL (EQ-5D) and Western Ontario and McMaster Universities Osteoarthritis Index (WOMAC). Radiographic knee OA was defined according to Kellgren/Lawrence (KL) grades, and symptomatic knee OA was defined as KL = 3 or 4 with knee pain. We also examined the independent association of symptomatic knee OA and grip strength with QOL.

Results: From the 3040 participants in the Research on Osteoarthritis Against Disability (ROAD) study, the present study analyzed 2126 subjects older than 40 years who completed the questionnaires (767 men and 1359 women; mean age, 68.9 ± 10.9 years). Subjects with KL = 3 or 4 had significantly lower physical QOL as measured by the physical component summary (PCS) score of the SF-8 and pain domains of the WOMAC, whereas mental QOL, as measured by the mental component summary (MCS) score of the SF-8, was higher in subjects with KL = 3 or 4 than KL = 0 or 1. Symptomatic knee OA was significantly more likely than radiographic knee OA without pain to be associated with physical QOL loss as measured by the PCS score and physical domains of the WOMAC. Symptomatic knee OA and grip strength were independently associated with physical QOL.

Conclusion: This cross-sectional study revealed that subjects with symptomatic knee OA had significantly lower physical QOL than subjects without it.

Introduction

Knee osteoarthritis (OA) is a major public health issue that causes chronic pain and disability[1–3]. The prevalence of radiographic knee OA is high in Japan[4], with 25,300,000 subjects aged 40 years and older estimated to experience radiographic knee OA[5]. According to the recent National Livelihood Survey of the Ministry of Health, Labour and Welfare in Japan, OA is ranked fourth among diseases that cause disabilities that subsequently require support with activities of daily living[6].

Quality of life (QOL) measurements in patients with chronic diseases are useful tools for estimating disease impact; these QOL scales may be generic or disease specific. Among the generic scales, the EuroQOL (EQ-5D) has been widely used to measure health-related QOL (HRQOL) in patients with OA[7,8], and several studies have used the Medical Outcomes Study Short Form-36 (SF-36) in

* Address correspondence and reprint requests to: Shigeyuki Muraki, Department of Clinical Motor System Medicine, 22nd Century Medical and Research Center, Faculty of Medicine, The University of Tokyo, Hongo 7-3-1, Bunkyo-ku, Tokyo 113-8655, Japan. Tel: 81-3-5800-9178; Fax: 81-3-5800-9179.
E-mail address: murakis-ort@h.u-tokyo.ac.jp (S. Muraki).

1063-4584/$ – see front matter
doi:10.1016/j.joca.2010.06.001

Caucasian patients with OA[9–11]. However, almost all of these studies include only patients with knee OA, and there are few population-based studies regarding knee OA and QOL[11]. A previous population-based study in Caucasians showed that arthritis has a major impact on the HRQOL measured by the SF-36 in a community setting[11], although arthritis was examined by self-reported means and not by radiographs. In terms of disease-specific scales for knee OA, the Western Ontario and McMaster Universities Osteoarthritis Index (WOMAC) has been used for Caucasians[12] and Asians[13,14], although these reports were not population-based studies. Furthermore, there is little information on the impact of knee OA with QOL in Japan, although a population survey suggests that the disease pattern differs among races[15–17]. In fact, the prevalence of knee OA in Japan[4] was much higher than that of previous epidemiologic studies in elderly Caucasians[16,18]. Furthermore, in terms of risk factors, studies in Caucasians have suggested that occupational activities that include kneeling and squatting were associated with knee OA[19], whereas these activities were not associated with Kellgren/Lawrence (KL) grades ≥ 2 OA in our previous study in Japan[20]. Therefore, the impact of knee OA on QOL also appears to differ in different populations. It would thus be of interest to clarify the impact of OA on QOL in a Japanese population.

The principal clinical symptom of knee OA is pain[21], but the correlation with the radiographic severity of knee OA is controversial[4,22–24]. Thus it would be interesting to determine whether the impact of radiographic knee OA on QOL differs according to the severity of OA. Furthermore, pain is strongly associated with QOL, so it would be of interest to clarify the impact of symptomatic OA as well as radiographic knee OA on QOL.

Gender differences have also been observed in knee OA. The prevalence of knee OA is higher in women than men[4], and the association of knee pain with knee OA also differs by gender[4]. Thus, the impact of these diseases on QOL may also differ between genders. However, to the best of our knowledge, there are no population-based studies that assess the association of knee OA with QOL in men and women separately.

Grip strength is a useful marker of muscle function and sarcopenia[25]. There is growing evidence that reduced grip strength is associated with adverse outcomes including morbidity[26], disability[27], falls[27], higher fracture rates[28], increased length of hospital stay[29], and mortality[27]. A previous study also showed that grip strength is related to total muscle strength[30]. Furthermore, there is increasing recognition that grip strength is a useful clinical marker of sarcopenia, and recent work has validated this approach, demonstrating that grip strength is more strongly associated with age and is a better predictor of poor mobility than other potential markers such as calf muscle area[31]. Previous reports have shown that low muscle mass was also associated with reduced QOL[32,33]; thus, the association of knee OA with QOL may be influenced by grip strength, but again, no studies have examined the association of knee OA and grip strength with QOL simultaneously in the same population.

The first objective of this study is to clarify the association of radiographic severity of knee OA with QOL among Japanese men and women using the large-scale, population-based cohort study called the Research on Osteoarthritis Against Disability (ROAD). Because pain is strongly associated with QOL, we also examined the association of symptomatic knee OA with QOL. Finally, we analyzed the independent associations of knee OA and grip strength with QOL.

Subjects and methods

Subjects

The ROAD study is a nationwide prospective study designed to establish epidemiologic indexes for evaluation of clinical evidence for the development of a disease-modifying treatment for bone and joint diseases (with OA and osteoporosis as the representative bone and joint diseases). It consists of population-based cohorts in several communities in Japan. A detailed profile of the ROAD study has been described in detail elsewhere[4,5,34]; a brief summary is provided here. To date, we have completed creation of a baseline database including clinical and genetic information for 3040 inhabitants (1061 men and 1979 women) ranging in age from 23 to 95 years (mean, 70.6 years), who were recruited from resident registration listings in three communities: an urban region in Itabashi, Tokyo, a mountainous region in Hidakagawa, Wakayama, and a seacoast region in Taiji, Wakayama. All participants provided written informed consent, and the study was conducted with the approval of the ethics committees of the University of Tokyo and the Tokyo Metropolitan Institute of Gerontology. Anthropometric measurements included height and weight, and body mass index (BMI) (weight [kg]/height^2 [m^2]) was calculated. Grip strength was measured on bilateral sides using a TOEI LIGHT handgrip dynamometer (TOEI LIGHT Co., Ltd, Saitama, Japan), and the better measurement was used to characterize maximum muscle strength. Among 2995 subjects aged 40 years or older in the ROAD study, 2243 (74.9%), 2245 (75.0%) and 2222 (74.2%) subjects completed the SF-8, the EQ-5D and the WOMAC, respectively, and 2126 (71.0%) subjects completed all three questionnaires. The present study analyzed 2126 subjects (767 men and 1359 women) aged 40 years (mean, 68.9 $\pm$ 10.9 years) or older who had completed the SF-8, the EQ-5D, and the WOMAC.

Radiographic assessment

All participants had radiographic examination of both knees using anterior–posterior and lateral views with weight-bearing and foot map positioning. Knee radiographs were read without knowledge of participant clinical status by a single well-experienced orthopaedist (SM) using the KL radiographic atlas for overall knee radiographic grades[35]. In KL grade, radiographs are scored as grade 0 through 4, with higher grades being associated with more severe OA. The higher KL grade in both knees was designated as that of the participant. Symptomatic knee OA was defined as: (1) a subject reporting knee pain lasting at least 1 month with pain having last occurred within the current or previous year; and (2) KL = 3 or 4 OA in the painful knee. To evaluate the intra-observer variability of KL grading, 100 randomly selected radiographs of the knee were scored by the same observer more than 1 month after the first reading. One hundred other radiographs were also scored by two experienced orthopaedic surgeons (SM & HO) using the same atlas for inter-observer variability. The evaluated intra- and inter-observer variabilities were confirmed by kappa analysis to be sufficient for assessment (0.86 and 0.80, respectively).

Instruments

The SF-8 generates a health profile consisting of eight scales and two summary measures describing HRQOL. The SF-8 is an alternate form to the SF-36, which is the most widely used patient-based health status survey, translated into more than 40 languages; the Japanese version of the SF-36 has been well validated[36]. The SF-8 uses a single question to measure each of the eight SF-36 domains. In the SF-8, each of the eight items assesses a different dimension of health: General Health (GH), Physical Functioning (PF), Role Physical (RP), Bodily Pain (BP), Vitality (VT), Social Functioning (SF), Mental Health (MH) and Role Emotional (RE). The SF-8 was scored by assigning the mean SF-36 scale score from the 2002 general Japanese population to each response category of the SF-8 measuring the same concept, and then weighting each SF-8 item to

compute aggregate physical component summary (PCS) and mental component summary (MCS) scores. The SF-8 may be scored using a published algorithm for Japanese versions of the SF-8, which has been well validated[37]. The EQ-5D self-report questionnaire measures five domains of HRQOL, including mobility, self-care, usual activities, pain/discomfort, and anxiety/depression[38]. Each of the five domains is assessed by a single question with three response levels (no problem, some problems, and extreme problems), so the EQ-5D defines a total of 243 health states. These results were coded and converted to a score of utility using the tables of values[39]. The EQ-5D scoring algorithm was first developed using time trade off-based preference scores for a sample of these health states from a representative sample of the UK general population[38]; the Japanese version of the EQ-5D has been validated[39]. This EQ-5D algorithm is used worldwide and generates scores ranging from −0.111 to 1.000, with negative scores representing health states worse than being dead, 0 representing being dead, and 1.00 representing a state of full health. The WOMAC, a 24-item OA-specific index, consists of three domains: pain, stiffness, and physical function. Each of these 24 items is graded on either a five-point Likert scale or a 100-mm visual analogue scale[12,40]. In the present study, we used the Likert scale (version LK 3.0). The domain score ranges from 0 to 20 for pain, 0 to 8 for stiffness, and 0 to 68 for physical function. Japanese versions of the WOMAC have also been validated[41].

Statistical analysis

The differences in age, height, weight, BMI, grip strength, and QOL measurements between men and women were examined by the Student's *t* test. The prevalence of radiographic and symptomatic knee OA was compared between men and women using the chi-square test. We also used the chi-square test to analyze whether subjects with one symptomatic knee were likely to have symptomatic OA in the other knee. According to KL grade[35], KL = 2 was defined as definite osteophytosis but no definite joint space narrowing, and KL = 3 and 4 included definite joint space narrowing. We thus categorized KL grade in KL = 0 or 1, KL = 2, or KL = 3 or 4, and differences among each KL grade with QOL measurements were determined using the Tukey Honestly Significant Difference (HSD) test without adjustment and after adjustment for age, BMI, and grip strength in men and women. We further classified subjects into those with symptomatic knee OA, those with KL = 3 or 4 knee OA without pain, and those without KL = 3 or 4 knee OA, and compared their association with QOL using the Tukey HSD test after adjustment for age, BMI, and grip strength. To determine the independent association of symptomatic knee OA and grip strength with QOL, we used multiple regression analysis without adjustment and after adjustment for age and BMI. Data analyses were performed using SAS version 9.0 (SAS Institute Inc., Cary, NC).

Results

The characteristics of the 2126 participants in the present study are shown in Table I. The prevalence of knee OA was significantly higher in women than men. The prevalence of bilateral and unilateral symptomatic knee OA was 2.0% and 3.0% in men, and 5.6% and 5.8% in women, respectively. Chi-square test showed that when the right knee had symptomatic knee OA, the odds ratio for the left knee to have symptomatic knee OA was 86.3 and 59.7 in men and women, respectively. The PCS and MCS of the SF-8 and the EQ-5D utility scores were significantly higher and the all domains of WOMAC were significantly lower in men than women, indicating that the QOL scores were higher in men than women.

Table I
Characteristics of participants

	Overall	Men	Women	*P*-Values
Number of subjects	2126	767	1359	
Age, years	68.9 ± 10.9	69.7 ± 10.5	68.4 ± 11.1	0.006
Height, cm	154.6 ± 9.2	162.8 ± 6.7	150.0 ± 6.9	<0.0001
Weight, kg	55.0 ± 10.9	61.5 ± 10.8	51.4 ± 9.0	<0.0001
BMI, kg/m^2	22.9 ± 3.6	23.1 ± 3.4	22.8 ± 3.7	0.03
Grip strength, kg	25.5 ± 9.3	33.2 ± 8.9	21.2 ± 6.3	<0.0001
Radiographic knee OA, %	17.9	11.6	21.5	<0.0001
Symptomatic knee OA, %	9.0	5.0	11.3	<0.0001
SF-8				
PCS	47.0 ± 7.0	47.4 ± 6.8	46.8 ± 7.0	0.03
MCS	52.8 ± 5.9	53.4 ± 5.3	52.5 ± 6.1	0.0009
EQ-5D	0.90 ± 0.15	0.91 ± 0.14	0.90 ± 0.15	0.03
WOMAC				
Pain (0–20)	1.37 ± 2.44	1.13 ± 2.16	1.50 ± 2.57	0.0003
Stiffness (0–8)	0.71 ± 1.25	0.63 ± 1.09	0.77 ± 1.33	0.01
Function (0–68)	4.08 ± 7.93	3.35 ± 7.06	4.49 ± 8.37	0.001

Except where otherwise indicated, values are the mean ± SD.
The differences between men and women were examined by the Student's *t* test except for the prevalence of radiographic and symptomatic knee OA.
The prevalence of radiographic and symptomatic knee OA was compared between men and women using the chi-square test.
Radiographic knee OA was defined as KL grade 3 or 4.
Symptomatic knee OA was defined as KL grade 3 or 4 with knee pain.
SF-8, Medical Outcomes Study Short Form-8.

The scores for PCS and MCS in the SF-8, the EQ-5D utility scores, and all domains in the WOMAC by KL grade of knee OA in men and women are shown in Tables II and III. The associations of age, BMI, and grip strength with each QOL parameter were significant in men and women by linear regression analysis ($P < 0.01$), except for the association of age with the MCS of the SF-8. Thus, we used the Tukey HSD test after adjustment for age, BMI, and grip strength to determine the association of radiographic severity of knee OA with QOL. Men and women with KL = 3 or 4 had significantly lower QOL measured by PCS of the SF-8 and pain domains of the WOMAC than those with KL = 0 or 1 as well as KL = 2. In addition, the MCS scores were higher in men and women with KL = 3 or 4 compared with KL = 0 or 1. The EQ-5D utility scores were not significantly associated with the KL grade of the knee after adjustment for age, BMI and grip strength.

Next, to determine impact of symptoms of radiographic knee OA with QOL, we classified subjects into those with symptomatic knee OA, defined as KL = 3 or 4 with knee pain, those with KL = 3 or 4 without pain, and those without KL = 3 or 4 and compared the impact of each type of OA on QOL using the Tukey HSD test after adjustment for age, BMI, and grip strength (Fig. 1). In men and women, PCS of the SF-8 and physical function domain of the WOMAC were significantly lower in subjects with symptomatic knee OA compared with those without KL = 3 or 4 knee OA (men: difference in mean −5.9, 95% CI −8.6 to −3.2 and difference in mean 4.9, 95% CI 2.2 to 7.6, respectively; women: difference in mean −4.3, 95% CI −5.7 to −2.9 and difference in mean 3.9, 95% CI 2.3 to 5.5, respectively) as well as KL = 3 or 4 knee OA without pain (men: difference in mean −6.3, 95% CI −9.7 to −3.0 and difference in mean 5.7, 95% CI 2.3 to 9.1, respectively; women: difference in mean −4.9, 95% CI −6.7 to −3.1 and difference in mean 3.9, 95% CI 1.8 to 5.9, respectively), whereas among those with KL = 3 or 4 knee OA without pain and no KL = 3 or 4 knee OA, there were no significant differences in PCS of the SF-8 and physical function domain of the WOMAC. In women, MCS of the SF-8 was significantly higher in subjects with symptomatic knee OA compared with those without KL = 3 or 4 knee OA (difference in mean 2.6, 95% CI 1.3 to 4.0) as well as KL = 3 or 4 knee OA without pain (difference in mean 2.3, 95% CI 0.6 to 4.0). The EQ-5D utility score was